9-12-2014

The State-Based Peridynamic Lattice Model

Raybea Richardson

Raybeau William Richardson
Candidate

Civil Engineering
Department

This thesis is approved, and it is acceptable in quality and form for publication:

Approved by the Thesis Committee:

Dr. Walter Gerstle , Chairperson

Dr. Arup Maji

Dr. Timothy Ross

THE STATE-BASED PERIDYNAMIC LATTICE MODEL

BY

Raybeau Richardson

B.S. Mechanical Engineering

University of New Mexico

THESIS

Submitted in Partial Fulfillment of the

Requirements for the Degree of

Master of Science

Civil Engineering

The University of New Mexico

Albuquerque, New Mexico, USA

July 2014

ACKNOWLEDGEMENTS

This thesis would not have been possible without the guidance of Dr. Walter Gerstle, the patience and support of my beautiful bride Annie, and the strength and grace of my Lord and Savior Jesus Christ.

'This is to my Fathers glory that you bear much fruit, showing yourself to by my disciples'

-John 15:8

THE STATE-BASED PERIDYNAMIC LATTICE MODEL

By

Raybeau Richardson

B.S., Mechanical Engineering, University of New Mexico, 2010

M.S., Civil Engineering, University of New Mexico, 2014

ABSTRACT

The reigning material model of today is continuum mechanics. Continuum mechanics assumes that a material is continuous and can be represented by mathematical functions. This is an unreasonable assumption for concrete due in part to the fact that concrete cracks and the continuum mechanics model cannot directly handle fracture.

In response to some of the limitations of continuum mechanics, Silling proposed a new method called peridynamics. Peridynamics assumes that a material is made up of particles which interact with each other via forces.

In this thesis we introduce the state-based peridynamic lattice model (SPLM) and describe its fundamental assumptions. SPLM discretizes a body into a finite number of particles that are arranged by a hexagonal close-packed lattice. We present a SPLM linear-elasticity and plasticity model that has been derived from the classical model. We then conclude this thesis with several benchmark examples and a look forward to future research.

Contents

List of Figures

List of Tables

Chapter 1

Introduction

1.1 Motivation

We are privileged to live in a time where the human race is the most technologically advanced it has ever been. Humanity has developed tools that allow us to study and understand the physical world to a greater degree than ever before. One fundamental tool that has been instrumental to these advancements is the modern day computer. The versatility and relatively limitless computational power of computers has forever changed the scientific community. With this tool, the author and many others are pushing past the boundaries of conventional theories and trailblazing new paths. However, before we get too far ahead of ourselves, we must first explain why a new material model is desirable.

The great engineering minds of the past, such as Newton, Euler, Bernoulli, Navier, Cauchy, etc., used the tool of their time to analyze structural members; that tool was calculus. In beam analysis for example, Euler and the Bernoulli brothers (who more mathematicians by today's standards) used differential calculus to develop relationships between displacement, slope, and curvature. This approach falls under the umbrella of classical mechanics. However there is a key assumption inherent to this approach: the beam deformation can be represented by a continuous function. At the time, these assumptions were reasonable because fatigue and fracture were not considered important.

As our understanding of the mechanics of material increased, mankind began to push the limits of engineering. However, it soon became clear that fatigue and fracture had to be considered, for example in the railroad business. In the 1800s bigger and stronger bridges were

required to accommodate the growing railroad industry. Railway bridges were subjected to cyclic dynamic loads imposed by heavy locomotives, thus iron beams and other metal components would quickly fluctuate between higher and lower states of stress. This produced fatigue fractures in metals and ultimately caused failures in some bridges. Therefore, in lieu of an accurate material model, structural members were designed with large factors of safety based on the static solution to reduce failures. Interestingly this is not very different from engineering practice today. Faced with these new challenges from growing industrial demands, scientists and engineers began to explore new theories to account for fatigue and fracture of materials.

In wasn't until the 1950s that fracture mechanics truly became an engineering discipline; this was due in part to the Liberty ship failures [1]. The Liberty ships were constructed with an all welded hull, as opposed to the traditional riveted hulls, allowing them to be produced quickly. The Liberty ships were hailed as a great success until in 1943 one of them broke completely in half. The Navy began to investigate and discovered that several hundred of the Liberty ships were showing signs of cracking. Because the hulls were essentially one large piece of metal cracks could propagate without much resistance. Thankfully most of the ships were able to be repaired with reinforcing plates. After World War II, researchers at the Naval Research Laboratory began investigate this problem in detail and formally created the field of fracture mechanics.

Fracture mechanics is really a subset of solid mechanics. Solid mechanics falls under the umbrella of continuum mechanics which is the study of the physics of continuous materials. Continuum mechanics assumes that a body completely fills the space it occupies and materials are still represented by continuous functions; however in contrast to the early theory of elasticity, continuum mechanics can model large deformations. Typically in continuum mechanics,

fracture mechanics is not even considered because by definition fracture represents a discontinuity in the material. To make fracture mechanics 'fit' into continuum mechanics all cracks must be redefined as boundaries of the body. Another fix to make fracture mechanics 'fit' is the use of stress intensity factors. Theoretically, using continuum mechanics, the stress at a sharp crack tip is infinite. No material can withstand infinite stress, thus stress intensity factors are used to calculate the stress intensity near a crack tip.

With this brief history in mind, there are several key points that argue for a new material model. First, the core assumption of these previous theories is that material behavior can be represented by continuous functions, thus materials have to be continuous. This is a reasonable assumption for crystalline structures like steel but is unreasonable for reinforced concrete. Typically, concrete members (columns, beams, and slabs) crack even before loads are applied to them, making them discontinuous. In the centuries past we needed the continuum assumption to be able to use differential calculus and functional analysis. However, today we have more tools available to us and differential calculus is not our only option. Second, engineering design is driven by code standards (e.g. ACI, AISC, etc.). These codes exist because we know that the theory is lacking. Therefore we impose factors of safety on our design to account for the unknown. Third, we have developed special case solutions for problems that cannot be solved using the traditional theory, particularly in the case of fracture mechanics. The author argues that these 'special cases' are a clear indicator that there is a flaw in the existing theory. Therefore, we go back to the basics and develop a model with alternate basic assumptions that are more suitable for the computer age.

1.2 Scope of thesis: SPLM

In this thesis we present a new material model call the State-based Peridynamic Lattice Model (SPLM). Contrary to continuum mechanics, SPLM assumes that a body is composed of a discrete and finite number of particles that interact with each other via forces. The foundations of a SPLM particle's motion are Newton's three laws:

1. A particle remains at rest or continues to move at a constant velocity, unless acted upon by an external force.
2. The vector sum of forces on a particle is equal to the mass of that particle multiplied by the acceleration vector of the particle.
3. When one particle exerts a force on a second particle, the second particle exerts a force equal in magnitude and opposite in the direction of the first particle.

SPLM relies on the power of computers for explicit calculation of Newton's Laws, hence the motion of particles, and makes no assumption of material continuity. While particles must move continuously in time, there is absolutely no physical law that says materials must deform continuously in space. This theory is the next step in the work of Silling, Gerstle, and others to create a better material model to be used in engineering practice [2, 3, 4, 7, 8, 9, and 13].

However, this thesis does not represent the full and completed SPLM theory. In this thesis we present the SPLM elasticity and plasticity models and do not address SPLM fracture or damage models.

1.3 Outline of thesis

This thesis includes eight chapters: Introduction, Background, Defining SPLM, Relationship between SPLM and Classical Mechanics, SPLM Linear Elasticity, SPLM Plasticity, Examples, and Conclusions.

Chapter Two provides a brief history and discussion of other relevant models. In this chapter we discuss classical mechanics, continuum mechanics, and Silling's peridynamic models in an effort to critically analyze the key assumptions made by each theory.

Chapter Three defines the key assumptions in SPLM, relevant terminology, and implementation. We discuss specific differences between SPLM and other theories as well as the lattice chosen to represent a SPLM material.

Chapter Four outlines the conditions for which a comparison between SPLM and classical mechanics can be made. When these conditions are met, we show that there is a kinematic relationship between SPLM stretch state and use energy considerations to develop the relationship between SPLM force state and classical stress.

Chapter Five focuses on the linear elastic relationship between SPLM link force state and stretch state. In this chapter we derive the linear micro-elastic material constants for 3D lattices and also the micro-elastic constants for the special 1D and 2D cases.

Chapter Six develops a SPLM plasticity model corresponding to the J2 plasticity model.

Chapter Seven presents several examples of SPLMs capability to model linear-elastic materials.

Chapter Eight provides a brief summary and a look forward to possible future research.

Chapter 2

Background

2.1 Introduction

For thousands of years people have been building structures using the materials and design tools that were available to them. Early structures were designed primarily by trial and error and were built using wood and stone. While these practices were more or less effective, people continued to search out new building methods for stronger, safer, and bigger structures. The application of mathematics has been a central tool in this pursuit, especially after Newton's contributions. Along with Newton's famous three laws of motion, he also invented the branch of mathematics called calculus which has provided many solutions to engineering problems. In the 1700s and 1800s engineers began to study and quantify the mechanics of deformable solids in mathematical terms.

However, these early pioneers were limited by their computational capabilities. At that time, all calculations had to be done by hand. This limitation forced models to be simplified so that they could be realistically applied in engineering practice. The development of modern electronic, digital computers has virtually eliminated this limitation in today's world. With this barrier gone, new models are being developed that are reinventing solid mechanics as we know it.

All models have their limitations. We must be conscious of their limitations in engineering practice. This chapter provides a brief description of some of these models as well as their limitations.

2.2 Classical mechanics

The first model we will discuss is the *classical mechanics* model. Classical mechanics describes the way bodies and forces interact with one another. The term classical mechanics can be used in reference to physics and mechanics of materials. Historically, classical mechanics originated in 1687 with Newtonian mechanics: the study of the relationship between mass, force, and acceleration [5]. Sir Isaac Newton first developed these relationships from observing the motion of the planets, moons, and other objects. However even before Newton, classical mechanics with respect to strength of materials really began with Galileo. In 1638, Galileo published his book 'Two New Sciences' in which he discussed, among other things, the mechanical properties of structural materials and even performed a strength analysis of a cantilever beam. While some of Galileo's ideas were later shown to be in error, his book represents the beginning of classical mechanics with respect to strength of materials. In the years that followed, there has been much advancement in the field of classical mechanics. However, we will discuss only a few of these most relevant to the research of this thesis. For a comprehensive history, refer to [12].

One of the key contributors to classical elastic theory was Navier. In the 1820's Navier made fundamental advancements in engineering and material science, specifically in the molecular theory of elastic bodies. An assumption in classical mechanics, one that had existed since the time of the Greek Philosophies, is that a solid body is actually comprised of many smaller particles or atoms (atom means 'indivisible' in Greek). Newton proposed that the properties of a body could be described in terms of the forces holding these particles together. Boscovich went on to say that between two particles in a body there exists a force that either

attracts or repels them. However, if the particles are too far apart, there is no force between them.

With these ideas in mind, Navier developed his own theory. He assumed that there are two sets of forces, $\sum F$ and $\sum F_1$, that act on a continuum of particles that make up an isotropic and linear elastic solid. $\sum F$ are the balanced molecular forces between particles when there are no external forces present. $\sum F_1$ are the internal forces required for particle equilibrium when external forces are imposed. Navier considers a single particle P, that is surrounded by other particles, that are then displaced by some small amount. Navier assumes that all particles within a sphere of action around P will exert forces on P due to this displacement. He then considers the force exerted on P from just one adjacent particle P_1. Navier proposes that this force, F_1, is proportional to the change in absolute distance, $r_1 - r$, between the two particles and multiplied by a weight factor, $f(r)$, that rapidly decreases as the particles get farther and farther apart:

$$F_1 = f(r)(r_1 - r). \tag{2.1}$$

Using a Cartesian coordinate system, Navier denotes u, v, and w as the components of displacement for particle $P(x, y, z)$ and $u + \Delta u$, $v + \Delta v$, and $w + \Delta w$ as the corresponding displacements of an adjacent particle $P_1(x + \Delta x, y + \Delta y, z + \Delta z)$. Therefore,

$$r_1 - r \approx \alpha \Delta u + \beta \Delta v + \gamma \Delta w \tag{2.2}$$

where α, β, and γ are the cosines of the angles which the direction r makes with the coordinate axis x, y, z. This force vector that acts on P is then decomposed into three vector components with respect to the Cartesian axis. Therefore, to find the total force exerted on P, the decomposed vector forces from all the particles within the sphere of action can be summed

together with respect to their corresponding Cartesian direction. We will introduce the following notation for brevity:

$$\theta = \frac{\partial u}{\partial x} + \frac{\partial v}{\partial y} + \frac{\partial w}{\partial z}\,, \tag{2.3}$$

$$\nabla = \frac{\partial^2}{\partial x^2} + \frac{\partial^2}{\partial y^2} + \frac{\partial^2}{\partial z^2}\,. \tag{2.4}$$

Navier's differential equations of equilibrium for isotropic, elastic bodies with material constant *C* are as follows:

$$C\left(\nabla u + 2\frac{\partial \theta}{\partial x}\right) + X = 0\,, \tag{2.5}$$

$$C\left(\nabla v + 2\frac{\partial \theta}{\partial y}\right) + Y = 0\,, \tag{2.6}$$

$$C\left(\nabla w + 2\frac{\partial \theta}{\partial z}\right) + Z = 0\,. \tag{2.7}$$

Navier's work was big step in the right direction, however we need to point out several of his key assumptions. First, he assumes that only one material constant, *C*, is needed for determining the elastic properties of a body. Second, Navier's body force equations require a continuous and differentiable displacement field. Lastly, these equations are not valid on or near the surface of the body. Recall that Navier assumes a sphere of action around a particle. At or near a surface there will not be a spherical volume of material surrounding each particle. Aware in part of this last limitation, Navier goes on to derive the equilibrium equations at the surface of the body that are in contact with the external forces. He denotes these boundary tractions as $\bar{X}_n$, $\bar{Y}_n$, and $\bar{Z}_n$ per unit area at some point on the surface with external normal *n*. To illustrate, $\bar{X}_n$ is as follows:

$$\bar{X}_n = C\left\{\left(3\frac{\partial u}{\partial x} + \frac{\partial v}{\partial y} + \frac{\partial w}{\partial z}\right)\cos\alpha + \left(\frac{\partial u}{\partial y} + \frac{\partial v}{\partial x}\right)\cos\beta + \left(\frac{\partial u}{\partial z} + \frac{\partial w}{\partial x}\right)\cos\gamma\right\} \tag{2.8}$$

where α, β, and γ define the orientation of the boundary surface. From Equation 2.8, we can see that Navier's surface forces are linear functions of the strain components! But at this time, stress and strain were not even defined. These notions, however, were not developed by Navier but by our next classical mechanics contributor.

Augustin Cauchy was an engineer turned mathematician whose work greatly impacted the field of mechanics. Around 1822 Cauchy became aware of Navier's work in elastic molecular theory, and became so interested that Cauchy himself began to work on that theory. Navier's theory related the force between particles to deformations in the body. Cauchy changes this idea: instead of particle force, he assumes that there is a force per unit area or pressure that acts upon a plane in the body. He calls this pressure a "tension or pression", thus introducing the idea of stress to the theory of elasticity. Using a tetrahedral element, Cauchy shows the three components of stress X_n, Y_n, and Z_n that act on the plane abc (Figure 2.1). These stress components are in terms of nine normal and tangential components of stress acting at O: σ_{xx}, σ_{yy}, σ_{zz}, τ_{xy}, τ_{xz}, τ_{yx}, τ_{yz}, τ_{zx}, and τ_{zy}. However, he goes on to prove that only six stresses are needed to define X_n, Y_n, and Z_n because $\tau_{xy} = \tau_{yx}$, $\tau_{xz} = \tau_{zx}$, and $\tau_{yz} = \tau_{zy}$.

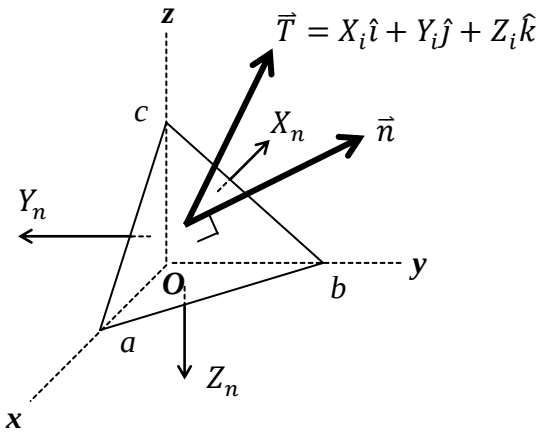

Figure 2.1, FBD of tetrahedral showing Cauchy Stress Components

Cauchy then performs a deformation analysis of an elastic body. His results showed that, for small deformations, the unit elongation in any direction and the change of the right angle between any two initially perpendicular directions can be described by six *strain* components: $\varepsilon_x = \frac{\partial u}{\partial x}$, $\varepsilon_y = \frac{\partial v}{\partial y}$, $\varepsilon_z = \frac{\partial w}{\partial z}$, $\gamma_{xy} = \frac{\partial u}{\partial y} + \frac{\partial v}{\partial x}$, $\gamma_{yz} = \frac{\partial v}{\partial z} + \frac{\partial w}{\partial y}$, and $\gamma_{xz} = \frac{\partial w}{\partial x} + \frac{\partial u}{\partial z}$. Cauchy also develops the constitutive equations for an isotropic elastic material that relates stress to strain. In these constitutive relationships, Cauchy again diverges from Navier's theory and proposes that two elastic constants are necessary to define these relationships. Cauchy's work not only fundamentally changed classical mechanics; it also provided the ground work for continuum mechanics.

Classical mechanics is widely used today in industry and engineering design. However, key simplifying assumptions are made, such as assuming deformations are small, to keep mathematical relationships simple yet meaningful. On the whole, the classical mechanics model works well, with respect to mechanics of materials, as long as stresses and strains remain within the elastic limit of the material and deformations are small. However, this model is not appropriate for large deformations, plasticity, fracture, and in such regimes, other models must be used. This brings us to our next section and the *continuum mechanics* model.

2.3 Continuum mechanics

Continuum mechanics is the analysis of the kinematic and kinetic behavior of materials modeled assuming continuous spatial behavior [6]. The continuum assumption states that a body completely fills the space that it occupies and may be divided into infinitesimally smaller and smaller particles that retain the material properties of the body as a whole. Each particle is then endowed with physical properties such as density, stress, strain, displacement, and velocity.

These physical properties are represented mathematically by analytic functions; thus the derivatives of these functions are also continuous. This assumption requires that any discontinuity must be defined as a boundary of the body for the continuum mechanics model to function correctly. Therefore, continuum mechanics model does not function well in the case of a growing discontinuity or a propagating crack. With these concepts in mind, we now briefly describe the key components of the continuum mechanics model.

To analyze deformation we limit our focus to just two particles in a body, as shown in Figure 2.2. Point 'P' on a body is represented in its undeformed, original state by vector $\boldsymbol{X}$ and the deformed, current state of point 'p' is represented by vector $\boldsymbol{x}$. We assume that there exists a differentiable and uniquely invertible function χ_i that maps x_i from the undeformed configuration to the deformed configuration in terms of $\boldsymbol{X}$,

$$x_i = \chi_i(\boldsymbol{X}). \qquad (2.9)$$

Now consider point 'Q' located $d\boldsymbol{X}$ from 'P'. After deformation, 'q' is now at a distance $d\boldsymbol{x}$ from 'p'. Because χ_i is assumed continuous, we can map the deformation between points from the undeformed to the deformed configurations,

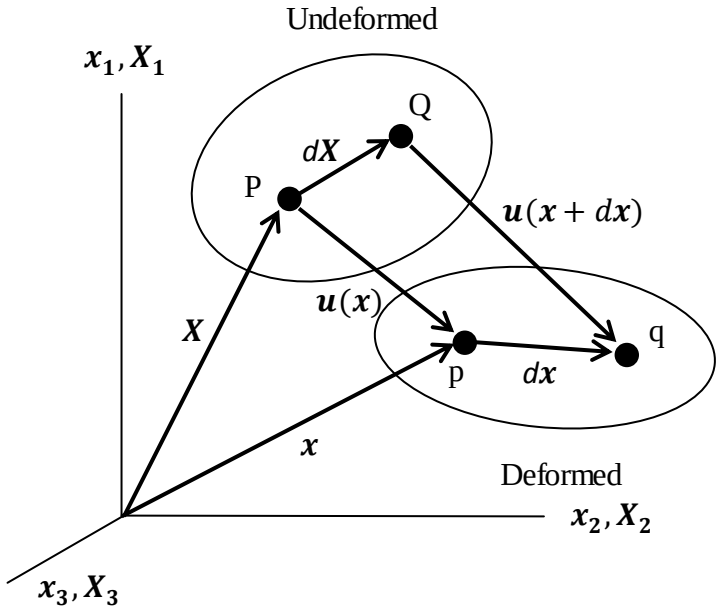

Figure 2.2 Vector $d\mathbf{X}$ between points P and Q in the undeformed configuration becomes $d\mathbf{x}$ between points p and q in the deformed configuration.

$$dx_i = \frac{\partial x_i}{\partial X_A} dX_A, \qquad (2.10)$$

where $\frac{\partial x_i}{\partial X_A}$ is commonly called the *deformation gradient* **F**. It can be shown that from **F**, the *Eulerian finite strain tensor* **e** can be found. Then using a linear constitutive relationship representative of the material, i.e. **C** for an elastic and isotropic material, the *Cauchy stress tensor* $\boldsymbol{\sigma}$ can be found at point 'p' in its current configuration, $\boldsymbol{\sigma} = \mathbf{Ce}$. To elaborate, $\boldsymbol{\sigma}$ defines the stress vectors acting on a surface with a unit normal $\hat{\mathbf{n}}$ on a cube of material at point 'p' in the deformed configuration. It is also possible to define equivalent stress vectors with a unit normal $\hat{\mathbf{N}}$ on that same cube of material at point 'P' in the undeformed configuration. This can be done by transforming $\boldsymbol{\sigma}$ into the *first Piola-Kirchhoff stress tensor* $\mathbf{P^o}$. For the full derivations of these concepts, refer to [5].

Continuum mechanics, in contrast to classical theory of elasticity, can model large deformations and plasticity, but this process it extremely complicated. In the case of large deformations, higher order terms cannot be assumed zero and must be accounted for. In the case of plasticity, the functions between stress and strain-rate become highly non-linear. Neither the continuum mechanics nor classical mechanics models can model fracture without additional theories – hence, the necessity for the discipline of fracture mechanics.

As building processes and computers have advanced, there is a growing need for models that can accurately predict fracture. Usually, structures and other solid materials are designed so that they will not exceed their elastic limits under the loads they are subjected too. But it is also important to be able to predict a structure's response if indeed the loads do exceed the elastic limit. Usually in engineering design, we want failures to occur slowly with obvious warning signs, not quickly and catastrophically. For example, reinforced concrete beams are designed to show visible signs of cracking and large deflections before they ultimately fail, in the hope that

this will allow the loss of life and property to be minimal. Currently, modeling discontinuities and fracture are not typically attempted because fracture mechanics theories are too complicated. Today's computers have advanced to the point where computational power is almost unlimited, however fracture theories remain complicated and hard to implement in the framework of continuum models. For example, modeling discontinuities with continuum mechanics is difficult because partial derivatives are used to calculate the relative displacement and force between two particles as previously described. If a 'spontaneous discontinuity' or crack is detected in a continuum mechanics model, the model must redefine the discontinuity as a boundary. Then a fracture or nonlocal damage mechanics approach must be used to simulate crack growth. Some models have been developed that attempt to do this type of modeling, but they are not very successful. In light of these limitations, a new theory was introduced by Silling in 2000 [8] called the *peridynamic* model.

2.4 Peridynamics

The name 'peridynamic' was proposed by Silling for this model from the Greek roots '*peri*', meaning near, and '*dynamic*', meaning force. Silling proposed a nonlocal continuum model that does not distinguish between points in the body where a discontinuity in displacement or any of its spatial derivatives may be located. This method falls into the category of a nonlocal model because particles separated by a finite distance (not just the immediate neighboring particles) can interact with each other. Silling's model relies on integration rather than differentiation to compute the forces on a particle. Therefore the equations that govern in Silling's peridynamic model are valid even at discontinuities in the deformation field. This approach is fundamentally different than previous theories. The first peridynamic theory, Silling's *bond-based* model, is discussed in the next section.

2.5 Bond-based peridynamics

In Silling's paper, [8], he introduces the bond-based peridynamic theory. Silling proposed that a body can be discretized into an infinite number of particles. These particles then interact with each other by means of a pairwise force function $\boldsymbol{f}$. The pairwise force function is the force vector per (unit volume squared) that a particle, with reference position $\boldsymbol{x'}$, exerts on another particle, with reference position $\boldsymbol{x}$, within a material neighborhood H_x as shown Figure 2.3. $\boldsymbol{f}$ is a function of relative position, $\boldsymbol{x'} - \boldsymbol{x}$, and relative displacement, $\boldsymbol{u}(\boldsymbol{x'}, t) - \boldsymbol{u}(\boldsymbol{x}, t)$, of two particles. Silling denotes relative position as $\boldsymbol{\xi} = \boldsymbol{x'} - \boldsymbol{x}$ and relative displacement as $\boldsymbol{\eta} = \boldsymbol{u}(\boldsymbol{x'}, t) - \boldsymbol{u}(\boldsymbol{x}, t)$. A key assumption of this model is that the $\boldsymbol{f}$ between two particles is completely dependent on $\boldsymbol{\xi}$ and $\boldsymbol{\eta}$, $\boldsymbol{f} = \boldsymbol{\mathcal{F}}(\boldsymbol{\eta}, \boldsymbol{\xi})$, and therefore completely independent the deformations of other surrounding particles. This $\boldsymbol{f}$ that acts between the two particles is equal, opposite, and collinear with the two particles so that no moment is applied either particle. Also, for a given material there is a positive number δ called the material horizon which defines the finite limit such that for any $|\boldsymbol{\xi}| > \delta$ the force between the two particles is zero, i.e. $\boldsymbol{f}(\boldsymbol{\eta}, \boldsymbol{\xi}) = \boldsymbol{0}$, $\forall \boldsymbol{\eta}, |\boldsymbol{\xi}| > \delta$. Assuming that particle $\boldsymbol{x}$ has a mass density ρ, Silling proposes that equation of motion for particle $\boldsymbol{x}$ is

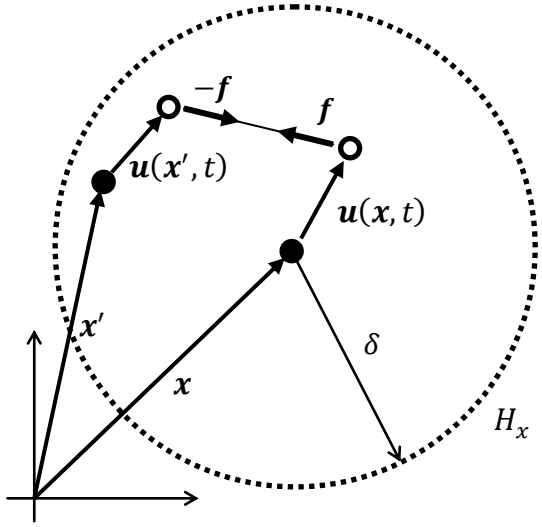

Figure 2.3 Bond-Based Model

$$\rho(\boldsymbol{x})\ddot{\boldsymbol{u}}(\boldsymbol{x}, t) = \int_{H_x} \boldsymbol{f}(\boldsymbol{\eta}, \boldsymbol{\xi}) dV_{x'} + \boldsymbol{b}(\boldsymbol{x}, t) \tag{2.11}$$

where **b** is the prescribed body force density field acting on the particle. The relative undeformed position vector $\boldsymbol{\xi}$ is called a 'bond'. The concept of bonds between particles acting over a finite distance is a fundamental difference between the peridynamic theory and the continuum mechanics theory.

Using the bond based peridynamic model Silling and others were able to develop models for practical application such as damage and failure in reinforced concrete under dynamic and quasi-static loading [2,3,4]. While this theory clearly shows potential, several limitations were discovered in implementation:

1. The peridynamic model defines the material in terms of pairwise force functions, not in terms of the continuum mechanics stress tensor. This is a practical barrier because the material model has to be recast in terms of pairwise force functions.
2. While plasticity can be modeled using the bond-based theory, the process causes volumetric strain which is unrealistic in metals.

In light of the difficulties, Silling made modifications to the bond-base theory and in 2007 he published a paper [9] that defined the *state-based* peridynamic theory which we will discuss next.

2.6 State-based peridynamics

In the state-based peridynamic model, Silling defines particle interactions in terms of 'force states' rather than in terms of pairwise force functions. Recall that in the bond-based method, $\boldsymbol{f}$ between two particles is a function dependent only on the relative positions, $\boldsymbol{\xi}$, and relative displacements, $\boldsymbol{\eta}$, of those two particles. Silling now proposes that the state of particle $\boldsymbol{x}$ is dependent on the states of all other particles $\boldsymbol{x}'$ within a spherical neighborhood $\mathcal{H}$ of radius δ.

These states are expressed by an infinite set of tensors. This set of tensors is denoted as $\mathcal{L}_m$ where m specifies the order. Therefore, Silling defines a state as the mapping of all $\boldsymbol{\xi}$ to tensors order m within a the spherical neighborhood:

$$\underline{\mathbf{A}}\langle\cdot\rangle : \mathcal{H} \to \mathcal{L}_m, \tag{2.12}$$

where the angle brackets refer to the vector, $\boldsymbol{\xi}$, on which the state operates. States of order 0 refer to a scalar state S and are written with an underscore and lowercase non-bold font, e.g. $\underline{a}$. States of order 1 refer to a vector state $\boldsymbol{V}$ and any state of order $m \geq 1$ is written with an underscore and uppercase bold font. While it is possible to have states of order $m > 1$, for the purposes of this thesis we will only be considering states of order 0, S, and 1, $\boldsymbol{V}$.

Recall that one of the limitations of the bond based model was that the model was in terms of pairwise force functions, $\boldsymbol{f}$, and not in terms of second order tensors. In the state-based model, the forces and deformations are expressed in terms of vector states which Silling argues are similar to second order tensors in that they both map vectors into vectors, but with three key differences:

1. A state is not in general a linear function of $\boldsymbol{\xi}$.
2. A state is not in general a continuous function of $\boldsymbol{\xi}$.
3. States are infinite dimensional.

In light of these differences, Silling develops two tools called *expansion* and *reduction*. The expansion tool $\underline{\mathrm{E}}$ is a function that expands a second order tensor $\mathbf{W}$ into an equivalent vector state,

$$\underline{\mathrm{E}}(\mathbf{W}) = \underline{\mathbf{W}}\langle\boldsymbol{\xi}\rangle \qquad \forall\boldsymbol{\xi} \text{ within } \mathcal{H}. \tag{2.13}$$

Conversely, the reduction tool $\mathcal{R}$ is a function that reduces a vector state of a particle to an approximately equivalent second order tensor,

$$\mathcal{R}\big(\underline{\mathbf{A}}\langle\boldsymbol{\xi}\rangle\big) = \mathbf{A} \qquad \forall \boldsymbol{\xi} \text{ within } \mathcal{H}. \tag{2.14}$$

To execute these functions, Silling first defines several terms. The first is the scalar *influence function* $\underline{w}\langle\boldsymbol{\xi}\rangle$. The influence function is chosen as non-negative in $\mathcal{H}$ and depends only on the magnitude of $\boldsymbol{\xi}$; thus it is said to be spherical. In other words, $\underline{w}\langle|\boldsymbol{\xi}|\rangle$ is a function that defines the influence of $\boldsymbol{x}'$ on $\boldsymbol{x}$, depending only on the distance between $\boldsymbol{x}'$ and $\boldsymbol{x}$.

Secondly, the *tensor product* creates a second order tensor from any two vector states,

$$\underline{\mathbf{A}}\langle\boldsymbol{\xi}\rangle * \underline{\mathbf{B}}\langle\boldsymbol{\xi}\rangle = \int_{\mathcal{H}} \underline{w}\langle\boldsymbol{\xi}\rangle \underline{\mathbf{A}}\langle\boldsymbol{\xi}\rangle \otimes \underline{\mathbf{B}}\langle\boldsymbol{\xi}\rangle dV_{\xi}, \tag{2.15}$$

where $\otimes$ is the dyadic product of the vector states.

The third term is the *reference position vector state* $\underline{\mathbf{X}}\langle\boldsymbol{\xi}\rangle$, which maps the relative undeformed position $\boldsymbol{\xi}$ for each particle to itself.

The last term necessary is the *shape tensor* $\mathbf{K}$, which is the tensor product of the reference position vector state $\underline{\mathbf{X}}\langle\boldsymbol{\xi}\rangle$ with itself,

$$\mathbf{K} = \underline{\mathbf{X}}\langle\boldsymbol{\xi}\rangle * \underline{\mathbf{X}}\langle\boldsymbol{\xi}\rangle. \tag{2.16}$$

Silling's expansion and reduction functions are as follows:

$$\underline{\mathcal{E}}(\mathbf{W}) = \underline{w}\langle\boldsymbol{\xi}\rangle[\mathbf{W}][\mathbf{K}]^{-1}\{\boldsymbol{\xi}\} = \underline{\mathbf{W}}\langle\boldsymbol{\xi}\rangle \tag{2.17}$$

and

$$\mathcal{R}\left(\underline{\mathbf{A}}\langle\boldsymbol{\xi}\rangle\right) = \left(\underline{\mathbf{A}}\langle\boldsymbol{\xi}\rangle * \underline{\mathbf{X}}\langle\boldsymbol{\xi}\rangle\right)[\mathbf{K}]^{-1} = \mathbf{A}. \tag{2.18}$$

However, in this authors opinion, Silling does not adequately show these relationships to be true. The reader of Silling's paper [9] is left to take Silling at his word that these expansion and reduction functions are valid. Nevertheless, with these tools in hand, Silling now describes his state-based model.

The state-based peridynamic model has three key states. The *force vector state field* $\underline{\mathbf{T}}$ describes the set of internal forces acting between particle $\boldsymbol{x}$ and all particles $\boldsymbol{x}'$. The *deformation vector state field* $\underline{\mathbf{Y}}$ describes the set of deformations, $\boldsymbol{y} = \boldsymbol{\xi} + \boldsymbol{\eta}$, for each particle $\boldsymbol{x}'$ with respect to the reference configuration of a particle. The scalar influence function $\underline{w}$ weighs the effect of one particle on another. There are two kinds of force states in the state based model,

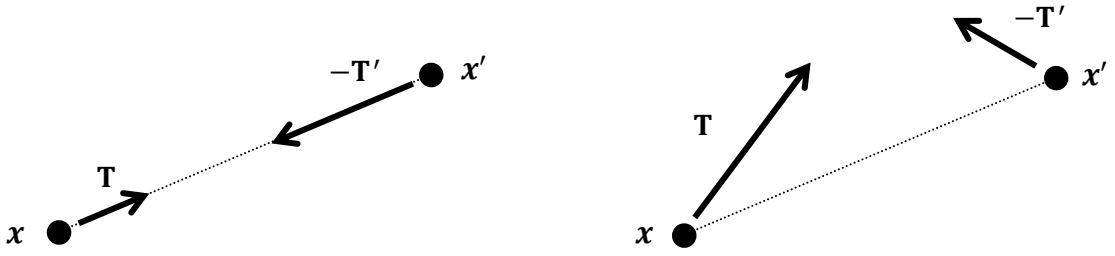

(a) Ordinary state based (b) Non-ordinary state based

Figure 2.4 Force States [9]

ordinary and *non-ordinary*, as shown in Figure 2.4.

In Silling's bond based theory, the equation of motion of a particle is a function of the pairwise force function between particles and the body force density field on the particle. The state based theory modifies the Equation 2.11 by replacing the pairwise force function with the force vector state field of the particle,

$$\rho\ddot{\boldsymbol{u}} = \int_{H_x} \{\underline{\mathbf{T}}\langle \boldsymbol{x}' - \boldsymbol{x}\rangle - \underline{\mathbf{T}}'\langle \boldsymbol{x} - \boldsymbol{x}'\rangle\} dV_{\boldsymbol{x}'} + \boldsymbol{b}. \tag{2.19}$$

To elaborate, the particle vector force (per unit volume), $\rho\ddot{\boldsymbol{u}}$, is equal to vector force state of $\boldsymbol{x}$ with respect to all $\boldsymbol{x}'$ within the material horizon, $\underline{\mathbf{T}}\langle \boldsymbol{x}' - \boldsymbol{x}\rangle$, minus the vector force states of all $\boldsymbol{x}'$ that act upon $\boldsymbol{x}$, $\underline{\mathbf{T}}'\langle \boldsymbol{x} - \boldsymbol{x}'\rangle$, integrated over the material horizon, H_x, all added to the body forces, $\boldsymbol{b}$. Generally speaking, the force state $\underline{\mathbf{T}}$ of a particle is a function of the deformation state $\underline{\mathbf{Y}}$ of the particle as well as possibly some other variables,

$$\underline{\mathbf{T}} = \mathcal{F}(\underline{\mathbf{Y}}, \Lambda). \tag{2.20}$$

Silling defines a material as 'simple' if the force state is a function of only the deformation state. In the rest of his paper, except with respect to plasticity, he assumes that all his materials are simple. Silling also shows in his paper that plastic incompressiblity in metals can be achieved using this method. We will now go through an example illustrating Silling's method.

Consider a body $\mathcal{B}$ that undergoes deformation, causing particle $\boldsymbol{x_i}$ to be displaced to $\boldsymbol{y_i}$, as shown in Figure 2.5. There could be any number, even an infinite number, of particles surrounding $\boldsymbol{x_i}$ that are within the material horizon. However, for clarity, only $\boldsymbol{x_i}$, $\boldsymbol{x_j}$ and $\boldsymbol{x_k}$ and their

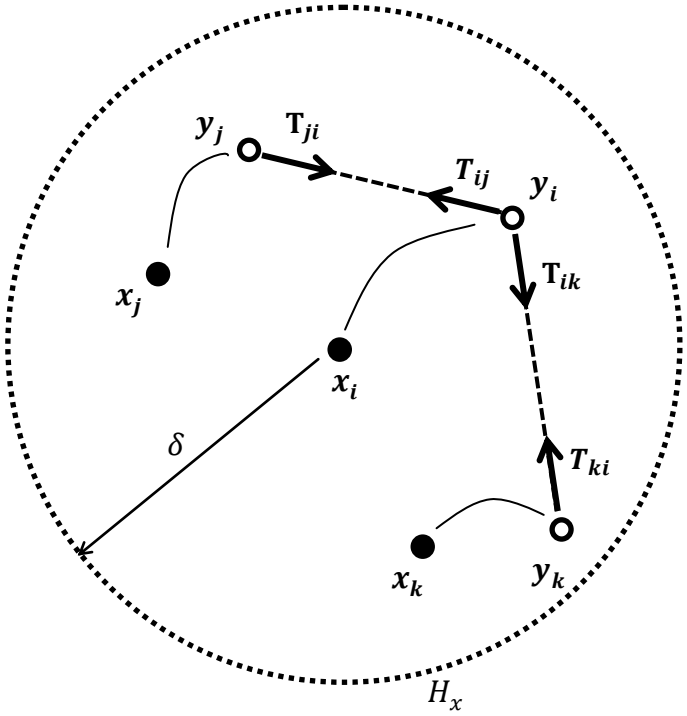

Figure 2.5 State-Based Model

respective displacements $\boldsymbol{y_i}$, $\boldsymbol{y_j}$ and $\boldsymbol{y_k}$ are shown. The deformation state of particle $\boldsymbol{x_i}$ is then defined as

$$\underline{\mathbf{Y}}\langle\boldsymbol{\xi}\rangle = \begin{Bmatrix} \boldsymbol{y_j} - \boldsymbol{y_i} \\ \boldsymbol{y_k} - \boldsymbol{y_i} \\ \vdots \\ \boldsymbol{y_\infty} - \boldsymbol{y_i} \end{Bmatrix} \quad \forall \boldsymbol{x} \in \mathcal{B}, \boldsymbol{\xi} \in \mathcal{H}. \tag{2.21}$$

Therefore, using Equation 2.18, we can reduce the vector deformation state to a second order tensor, $\mathcal{R}\big(\underline{\mathbf{Y}}\langle\boldsymbol{\xi}\rangle\big) = \mathbf{Y}$. Silling then shows in [9] that the reduced peridynamic state, $\mathbf{Y}$, is approximately equal to the corresponding continuum mechanics deformation gradient tensor, $\bar{\mathbf{F}}$. With the deformation gradient known, the corresponding first Piola-Kirchhoff stress tensor $\mathbf{P^o}$ can be found using the standard continuum mechanics process outlined in Section 2.3. Knowing $\mathbf{P^o}$, we expand the corresponding force state $\underline{\mathbf{T}}$ for particle $\boldsymbol{x}$ using Equation 2.17,

$$\underline{\mathbf{T}}\langle\boldsymbol{\xi}\rangle = \underline{\mathcal{E}}(\mathbf{P^o}) \,. \tag{2.22}$$

With this general approach, Silling was able to remove the limitations previously mentioned in his bond-based model, creating a model that is even more general than the continuum model.

Silling's state-based peridynamic model, while groundbreaking, has several arguable limitations. First of all, Silling's theory is general to a fault. It leaves the user to define model parameters such as the material horizon, the influence function, how the particles are arranged, and other specifics. Also, because the problem has to be discretized prior to computational simulation, a convergence study is necessary. In this writer's opinion, engineers need more prescribed methods of modeling.

A philosophical argument can made that the peridynamic model does not need to be dependent on a continuum approach. Silling assumes that a body is composed of an infinite

continuum of particles, same as the continuum model. Then, using the state-based theory, Silling reduces the deformation state into an average deformation gradient tensor, uses a continuum mechanics approach to find the stress tensor, and then expands the stress tensor to find the corresponding force state. We agree that, when possible, there should be correspondence between the peridynamic model and the continuum mechanics model; both models should give the same results in simple cases where the solution is known, i.e. a bar in uniaxial tension should have a yield force state that corresponds with the equivalent measured yield stress. However, we argue that it is unnecessary to compare peridynamics with continuum mechanics. By comparing these two theories, you make that assumption that continuum mechanics method is correct and the peridynamic method is just a variant of continuum mechanics to help model discontinuities. Why can't we leave continuum mechanics and build an independent peridynamic model? With the advancement of computer processing power, why can't we model structures with a finite number of particles? We are not discounting the merits of the continuum model, but we claim that the peridynamic model need not rely on continuum theory. We will explore this idea further in later chapters of this thesis.

Even with these arguable flaws, Warren, Silling, Askari, Weckner, Epton, and Xu [13] have implemented Silling's state-based peridynamic theory. We will go over this implementation in the next section.

2.7 Non-Ordinary State-Based Peridynamic Computational Implementation

In 2009, Warren, Silling, Askari, Weckner, Epton, and Xu published a paper in the International Journal of Solids and Structures [13] where they implement Silling's state-based peridynamic method into a dynamic computer model. Using Silling's and Askari's three-

dimensional peridynamic modeling code, EMU, they discretize a body into a cubic lattice of particles. Every particle has an identifier j, position $\mathbf{x_j}$, and volume V_j in the reference configuration. Silling's state based peridynamic equation of motion is then solved using Riemann sums;

$$\rho(\mathbf{x_j})\ddot{\boldsymbol{u}}(\mathbf{x_j},t) = \sum_{n=1}^{m}\{\underline{\mathbf{T}}[\mathbf{x_j},t]\langle\mathbf{x_n}-\mathbf{x_j}\rangle - \underline{\mathbf{T}}[\mathbf{x_n},t]\langle\mathbf{x_j}-\mathbf{x_n}\rangle\}V_n + \boldsymbol{b}(\mathbf{x_j},t) \qquad j = 1,2,\dots,q \tag{2.23}$$

where j corresponds to the node number, m is the number of unbroken bonds that connect to node j, and q is the total number of nodes or particles in the system as well as the number of equations generated. Then, the q number of equations are solved explicitly using a central difference time integration method. To ensure stability, they calculate a critical time step approximated by the transit time of a dilatation wave over the shortest length scale in the system as described by Taylor and Flanagan [11]. However, in this case they use the length scale controlled by the material horizon rather than the lattice spacing (which is smaller than the material horizon). They acknowledge this deviation from Taylor and Flanagan's method in the paper and state that the approximate critical time step they calculate is, in most cases, not conservative. Therefore, they use a time step smaller than the calculated time step.

They then formulate a solution for finite deformation problems using the non-ordinary state-based peridynamic method. The model is assumed to be non-ordinary because, in general, the bond forces are not collinear with bond deformation. A scalar influence function of unity is selected to weight the effects of points $\mathbf{x_n}$ on point $\mathbf{x_j}$ (all $\mathbf{x_n}$ are within the material horizon of $\mathbf{x_j}$). Silling's reduction formula, Equation 2.18, is modified to be expressed as a Riemann sums,

$$\mathbf{F}(\mathbf{x_j}) = \left[\sum_{n=1}^{m} w(|\mathbf{x_n} - \mathbf{x_j}|)\left(\underline{\mathbf{Y}}\langle \mathbf{x_n} - \mathbf{x_j}\rangle \otimes (\mathbf{x_n} - \mathbf{x_j})\right) V_n\right] \cdot \mathbf{B}(\mathbf{x_j}) \,,$$

(2.24)

where

$$\mathbf{B}(\mathbf{x_j}) = \left[\sum_{n=1}^{m} w(|\mathbf{x_n} - \mathbf{x_j}|)\left((\mathbf{x_n} - \mathbf{x_j}) \otimes (\mathbf{x_n} - \mathbf{x_j})\right) V_n\right]^{-1} .$$

(2.25)

From this average deformation gradient calculated at point $\mathbf{x_j}$, a continuum mechanics approach is used to obtain the Lagrangian strain tensor. Bond rupture is defined as a function of the second invariant of the deviatoric strain tensor and the average volumetric strain. A von Mises elastic-plastic isotropic linear hardening model with an associated flow rule was chosen as the constitutive model. Therefore, the equivalent Cauchy stress tensor is determined and then expanded to the corresponding force state. This approach is modeled on a three dimensional bar in uniaxial tension and the results are compared to the analytical solution. The following conclusions about this method are made based on these examples:

- Analysis of the bar in uniaxial tension with varying lattice rotations deforms in agreement with the analytical method.
- If uniaxial tension applied very slowly, it will produce homogeneous deformation along the entire bar.
- Uniaxial tension is applied to a bar with a notch in the center, demonstrating the fracture and damage capabilities of this method. The results of which match very closely with the analytical solutions.

To the authors' credit, they successfully implemented Silling's state based peridynamic method. However the limitations of Silling's model, as discussed at the end of the previous section, are clearly illustrated throughout this paper. It was left to the authors to define all the model parameters (material horizon, influence function, ect.) as well as to develop a step by step procedure to implement this method. As we stated before, this burden will send users seeking other more prescribed methods. Also, this computer implementation method still relies heavily on continuum mechanics. For every time step, the peridynamic model is reduced to a continuum model, analyzed with a continuum mechanics approach, and then expanded back to update the peridynamic model. We argue, as in the previous section, that a purely peridynamic approach can be used to simply and accurately model elasticity, plasticity, damage, and fracture.

2.8 Summary

In this chapter we have presented a brief overview of the history of models that help quantify the strength of materials as well as some of their limitations. Despite these limitations, these models have helped shape and grow our understanding of the physical world. The author acknowledges and is thankful for the contributions made by these great people and the work they have done. We do not seek to 'trample' on their models with our criticism. Our objective is to improve the existing models by honestly defining their limitations and seeking solutions. This is what all the authors of these various models have done, and we are better for it. In this spirit, we now devote the rest of this thesis to describing a new *state-based peridynamic lattice model*, or SPLM.

Chapter 3

Defining SPLM

3.1 Introduction

In this chapter we define the State-Based Peridynamic Lattice Model (SPLM). SPLM is a new material model that takes advantage of the recent computational power available to us to simply and accurately predict material behavior. In the previous chapter we reviewed several other material models, but we want to specifically compare SPLM to classical mechanics and Silling's state-based peridynamic model.

Classical mechanics assumes that a body is homogeneous and that its physical properties can be represented by continuous mathematical functions; any discontinuity must be defined as a boundary. Thus, this approach is only valid when a spatially continuous displacement field can be assumed. SPLM is not bound by this restriction and is therefore more general than classical mechanics. Silling's state-based peridynamic model, however, is bound by the reference material continuum assumption. In his theory, Silling outlines a method that can approximate a corresponding deformation gradient tensor from a state-based deformation state. Silling's state-based peridynamic approach can therefore be used to model elasticity, plasticity, and fracture. However, his approach is so general that it leaves the user to determine a deterring number of model parameters. In this sense, SPLM is less general than Silling's state-based model, but designed to be more user friendly.

With SPLM, a solid body is modeled as a finite number of particles arranged in a regular lattice. These particles have a specified mass and interact with their neighboring particles via peridynamic-bond forces, or *pd-bond forces* for short. We assume that these pd-bond forces are

a function of the *pd-bond stretches* of all neighboring particles. In the remainder of the chapter we will define the key assumptions of SPLM, differences between SPLM and other models, and specific model parameters of SPLM.

3.2 The lattice

SPLM assumes that a material is represented by a lattice of particles. This is a key difference between SPLM and Silling's peridynamic model. Silling's model assumes that particles in the reference configuration are in three dimensional space, $\mathcal{R}^3$. However, in the implementation of Silling's peridynamic model, an infinite number of particles need to be arranged in some fashion. Particles *could* be randomly arranged; however this would be very computationally expensive. Silling's own peridynamic computer program, EMU, arranges particles using a cubic lattice. SPLM assumes that particles are arranged in a lattice and thus the lattice is fixed. Note that any lattice could be chosen for SPLM, even a random lattice. A hexagonal close packed (HCP) lattice shown in Figure 3.1 has been chosen for SPLM because it offers a high degree of symmetry and density of particles. For a history of lattice modeling, refer to [7].

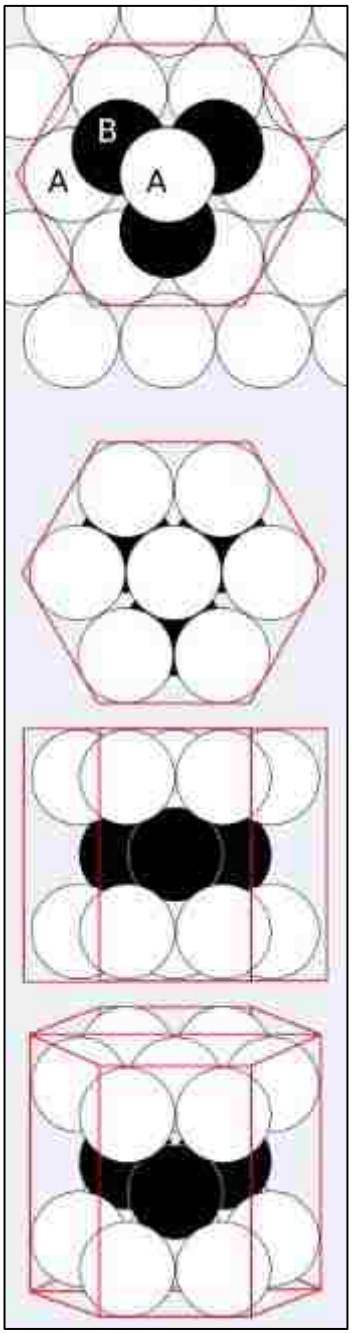

Figure 3.1 HCP Lattice from http://en.wikipedia.org/wiki/Close-packing_of_equal_spheres

By assigning a HCP lattice in SPLM, this assumption also introduces another property inherent of the material. In isotropic linear elasticity, a material is generally represented by just two

properties; the modulus of elasticity E and Poisson's ratio ν. A SPLM isotropic linear elasticity material has both of these properties as well as lattice spacing, L, for a total of three material constants.

3.3 The particles

SPLM assumes that any elasto-plastic solid can be represented as a finite number of individual particles. The particle mass is a model parameter of SPLM and will be chosen by the user. The user has the freedom to choose the particle mass with respect to the lattice spacing, L, of the solid being modeled. For example, the particle mass used to model a dam may be larger than the particle mass chosen to model a beam. This model parameter has one restriction: the lattice spacing is to be no smaller than largest 'component' of the material being modeled. For example, the smallest lattice spacing possible when modeling concrete is the average aggregate size. Similarly, the smallest particle size possible when modeling metals is the average grain size. This restriction places a realistic lower limit on the lattice spacing used in SPLM and is physically reasonable. To ensure isotropy, we assume that a particle interacts with its twelve nearest neighboring particles (Figure 3.2(i)) as well as its six second-nearest neighbors (Figure 3.2(ii)). The nearest neighboring pd-bonds are of length L and the second nearest neighboring pd-bonds are of length $\sqrt{2}L$. Therefore, any given SPLM particle has a total of eighteen pd-bonds. Table 3.1 shows the pd-bond ID and the location of the neighboring particle that the pd-bond connects with. Because of the lattice arrangement, the "tributary volume" (shown in Figure 3.2) of a particle is actually a rhomboid,

$$\Delta V = (L)\left(\frac{\sqrt{3}}{2}L\right)\left(\sqrt{\frac{2}{3}}L\right) = \frac{L^3}{\sqrt{2}}. \tag{3.1}$$

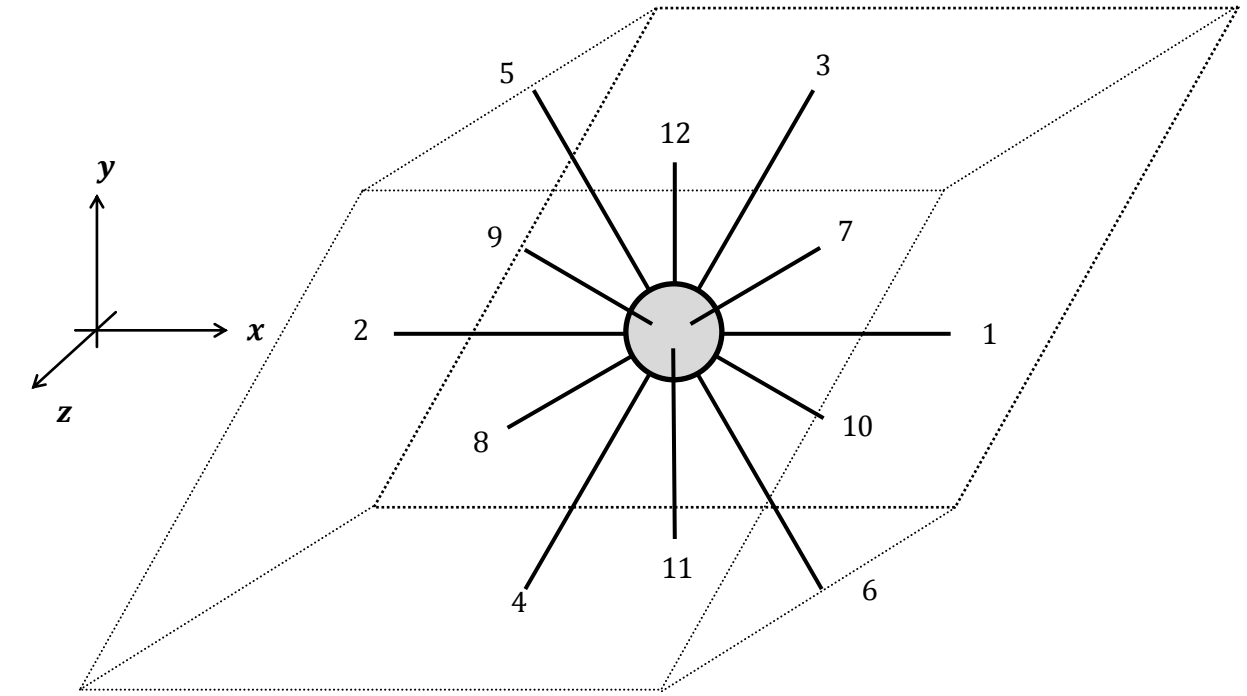

(i) 12 nearest neighboring pd-bonds

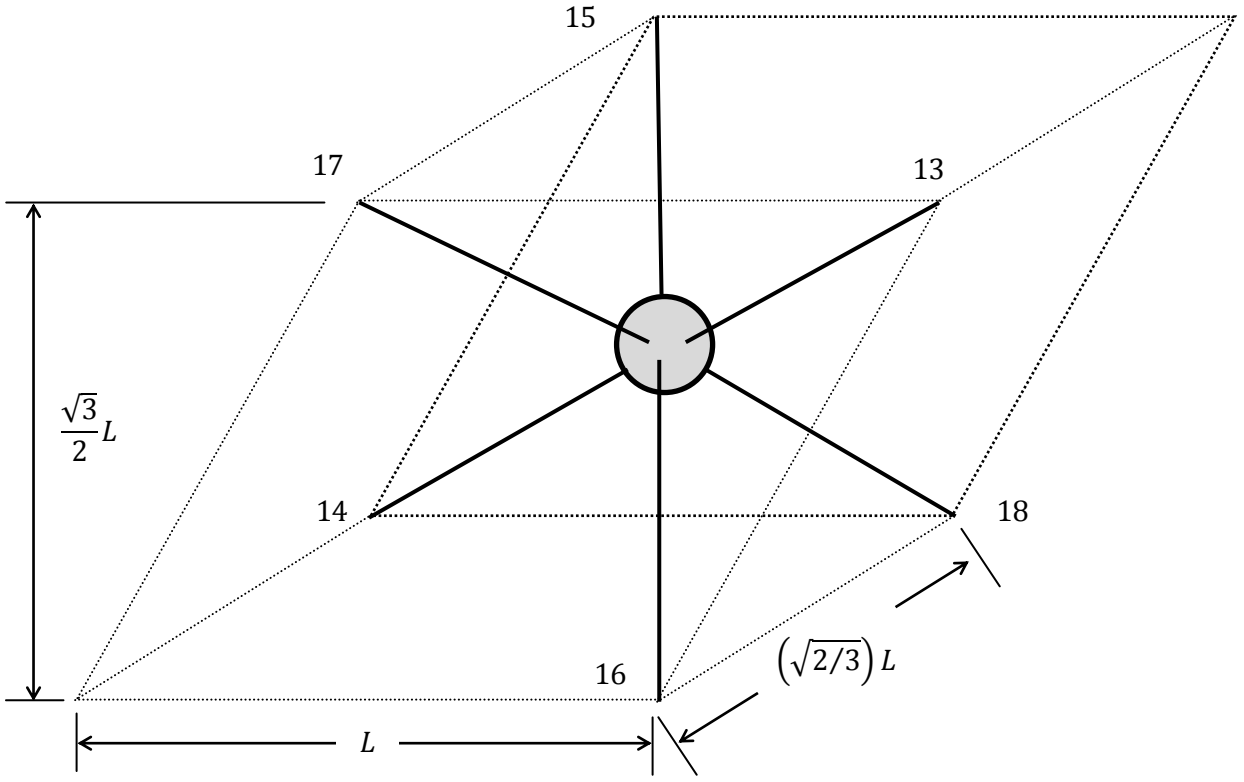

(ii) 6 second nearest neighboring pd-bonds

Figure 3.2 3D particle tributary volume and pd-bonds

pd-bond ID	X	Y	Z
1	L	0	0
2	$-L$	0	0
3	$L/2$	$\sqrt{3}L/2$	0
4	$-L/2$	$-\sqrt{3}L/2$	0
5	$-L/2$	$\sqrt{3}L/2$	0
6	$L/2$	$-\sqrt{3}L/2$	0
7	$L/2$	$\sqrt{3}L/6$	$\sqrt{6}L/3$
8	$-L/2$	$-\sqrt{3}L/6$	$-\sqrt{6}L/3$
9	$-L/2$	$\sqrt{3}L/6$	$\sqrt{6}L/3$

pd-bond ID	X	Y	Z
10	$L/2$	$-\sqrt{3}L/6$	$-\sqrt{6}L/3$
11	0	$-\sqrt{3}L/3$	$\sqrt{6}L/3$
12	0	$\sqrt{3}L/3$	$-\sqrt{6}L/3$
13	$-L$	$-\sqrt{3}L/3$	$\sqrt{6}L/3$
14	L	$\sqrt{3}L/3$	$-\sqrt{6}L/3$
15	0	$2L/\sqrt{3}$	$\sqrt{6}L/3$
16	0	$-2L/\sqrt{3}$	$-\sqrt{6}L/3$
17	L	$-\sqrt{3}L/3$	$\sqrt{6}L/3$
18	$-L$	$\sqrt{3}L/3$	$-\sqrt{6}L/3$

Table 3.1, pd-bond coordinates

3.4 pd-bond force state, $\{\boldsymbol{T}\}$

Newton's third law states that when one body exerts a force on a second body, the second body simultaneously exerts a force equal in magnitude and opposite in direction on the first body. Therefore, we require that forces between particles satisfy this law. SPLM defines the *pd-bond forces state,* $\{\boldsymbol{T}\}$, to be an 18x1 matrix that represents one half the force in the pd-bonds surrounding the particle,

$$\{\boldsymbol{T}\} = \begin{Bmatrix} F_1 \\ F_2 \\ \vdots \\ F_{18} \end{Bmatrix}. \tag{3.2}$$

Consider Figure 3.3 which shows a particle surrounded by its six in-plane nearest neighbors (other out-of-plane pd-bonds are not shown for clarity). The forces between particles are in line with the direction of the pd-bonds, therefore we consider the pd-bonds force state to be a vector state. It is possible for the force between particles to be unequal (i.e. $f_4 \neq f_4{}'$) thus we average

the forces between particles to satisfy Newton's third law. Therefore, the total vector force state, $\{\boldsymbol{F}\}$, of the particle is

$$\{\boldsymbol{F}\} = \{\boldsymbol{T}\}\langle \boldsymbol{x}, \boldsymbol{x}' \rangle - \{\boldsymbol{T}'\}\langle (\boldsymbol{x}', \boldsymbol{x}) \rangle. \tag{3.3}$$

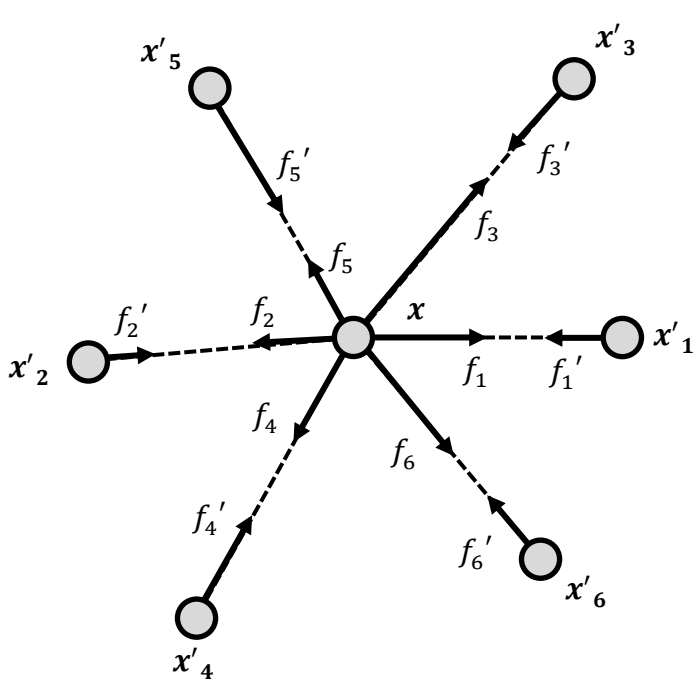

$$F_1 = \frac{f_1}{2}$$

$$F_2 = \frac{f_2}{2}$$

$$F_3 = \frac{f_3}{2}$$

$$F_4 = \frac{f_4}{2}$$

$$F_5 = \frac{f_5}{2}$$

$$F_6 = \frac{f_6}{2}$$

Figure 3.3 In-plane SPLM pd-bond force state

3.5 pd-bond stretch state, $\{\boldsymbol{S}\}$

SPLM defines the *pd-bond stretch state* to be an 18x1 matrix that represents the stretch of the pd-bonds surrounding the particle,

$$\{\boldsymbol{S}\} = \begin{Bmatrix} S_1 \\ S_2 \\ \vdots \\ S_{18} \end{Bmatrix}. \tag{3.4}$$

Consider Figure 3.4 which shows the pd-bonds stretches for the in-plane pd-bonds. We define the stretch of a pd-bonds to be the change (with respect to the reference configuration) in the pd-bond's length, ΔL_i, divided by the reference pd-bond length, L_i,

$$S_i = \frac{\Delta L_i}{L_i}. \tag{3.5}$$

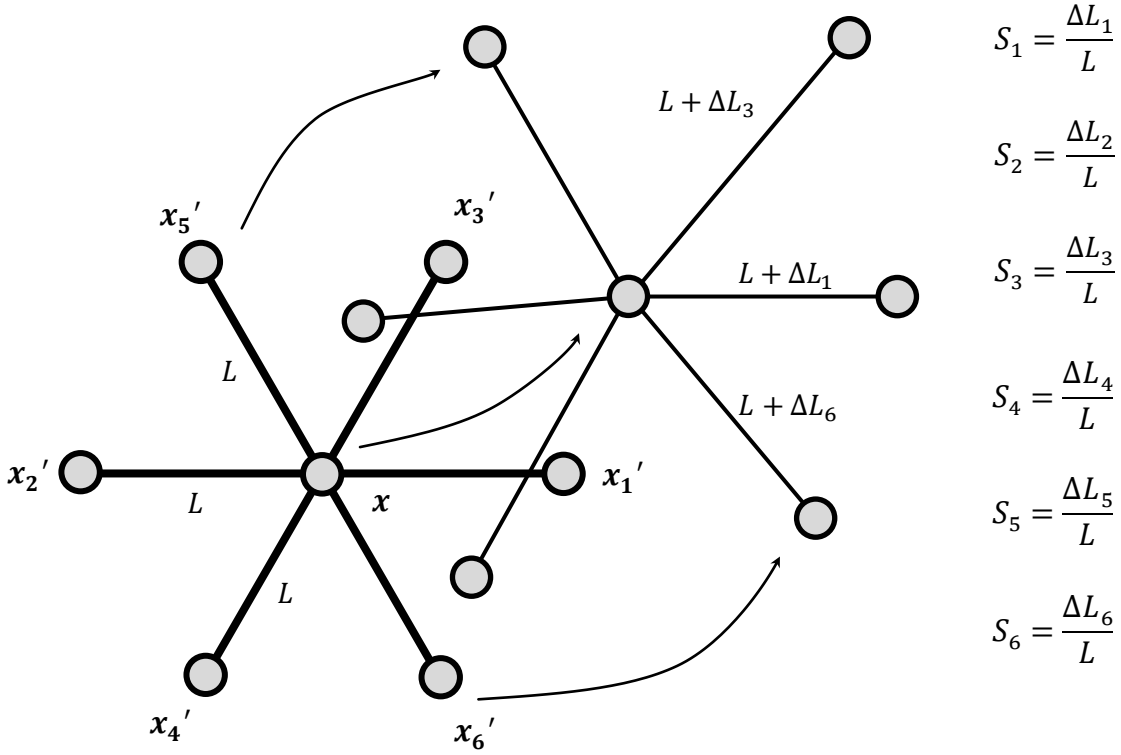

Figure 3.4 In-plane SPLM pd-bond stretch state

Similar to the pd-bond force state, the pd-bond stretches have inherent direction because they are in line with the pd-bonds, thus we consider them to be vectors. In this thesis, we assume the pd-bond force state of a particle is a function of the pd-bond stretch state of that particle,

$$\{\boldsymbol{T}\} = f(\{\boldsymbol{S}\}) \tag{3.6}$$

3.6 SPLM for one and two dimensions

SPLM is a fully three dimensional model. However, for computational efficiency, SPLM can also model one- and two-dimensional problems. We consider one- and two-dimensional problems to be special cases of the three-dimensional problem. Therefore, when simplifying assumptions can be made, we can represent a three dimensional particle as a one dimensional lattice *strand* of particles or by a two dimensional lattice *layer* of particles. A lattice strand of

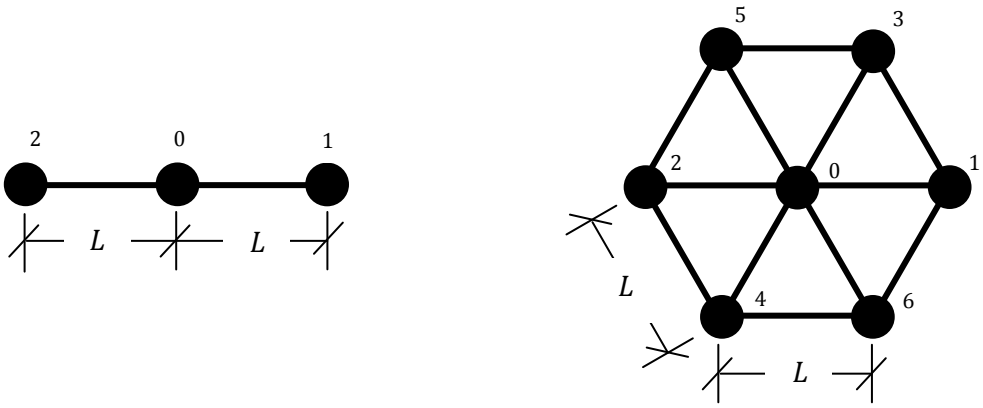

(i) 1D strand (ii) 2D layer

Figure 3.5 1D and 2D SPLM

particles is a tributary row of three-dimensional particles representative of a three-dimensional body. The forces applied to the tributary area of a strand of particles are proportion to the area of the three-dimensional body. A lattice layer is a tributary plane of three dimensional particles representative of a three dimensional body. Similar to the strand of particle, the forces applied to the tributary thickness of a layer of particles are proportion to the thickness of the three-dimensional body. In both cases, the particles still have eighteen links each.

3.7 Summary

In this chapter we have defined the fundamentals of SPLM as well as pointing out some of the specific difference between SPLM and other models. SPLM assumes that particles are arranged in a HCP lattice. Each particle has eighteen pd-bonds that connect to its nearest and second nearest neighbors. The forces in the pd-bonds surrounding a particle are called the pd-bonds force state and the stretches of those pd-bonds are called the pd-bonds stretch state. For the purposes of this thesis we have chosen to define the pd-bond force state and pd-bond stretch state as specified in sections 3.4 and 3.5. However, other criteria could be used to define SPLM states. When possible, a three-dimension body can be represented by a tributary one-dimensional lattice strand or two-dimension lattice layer of three-dimensional particles. As we compare SPLM to classical mechanics and define SPLM elasticity and plasticity we will draw on the terminology defined in this chapter.

Chapter 4

Relationship between SPLM and Classical Mechanics

4.1 Introduction

In this chapter we derive, to the extent possible, the relationship between classical mechanics and the state-based peridynamic lattice model (SPLM) assuming small deformations and spatially homogeneous strain. SPLM is distinctly different from classical mechanics. That being said however, it is useful for us to relate SPLM to the classical model where possible. But we must be clear that this relationship is only valid under certain conditions. Classical mechanics of deformable bodies assumes a continuous, differentiable displacement field and a continuous reference configuration. SPLM is not bound by these assumptions, although for the purposes of this thesis, we assume that deformations are small. For a comparison to be made, we require that classical stress and strain and the corresponding SPLM pd-bond force state and pd-bond stretch state be energy-equivalent. When these conditions are met, we can derive the relationship between SPLM and the classical model.

There are differences between the models that we need to be aware of in the development of these relationships. Consider a three-dimensional body subjected to loading by arbitrary external forces, shown in Figure 4.1. Let us analyze a small piece, ΔV, of the interior of this object using both models. Using the classical model we consider the stress $\{\boldsymbol{\sigma}\}$, assumed homogeneous within ΔV, with six components of stress: σ_{xx}, σ_{yy}, τ_{xy}, σ_{zz}, τ_{yz}, and τ_{zx} (σ_{zz}, τ_{yz}, and τ_{zx} are omitted from Figure 4.1 for clarity). Using SPLM, we define the pd-bond force state $\{\boldsymbol{T}\}$ of an equivalent particle with eighteen components of force (pd-bond forces F_{13} through F_{18} are omitted from Figure 4.1 for clarity). In matrix form, these states are expressed as

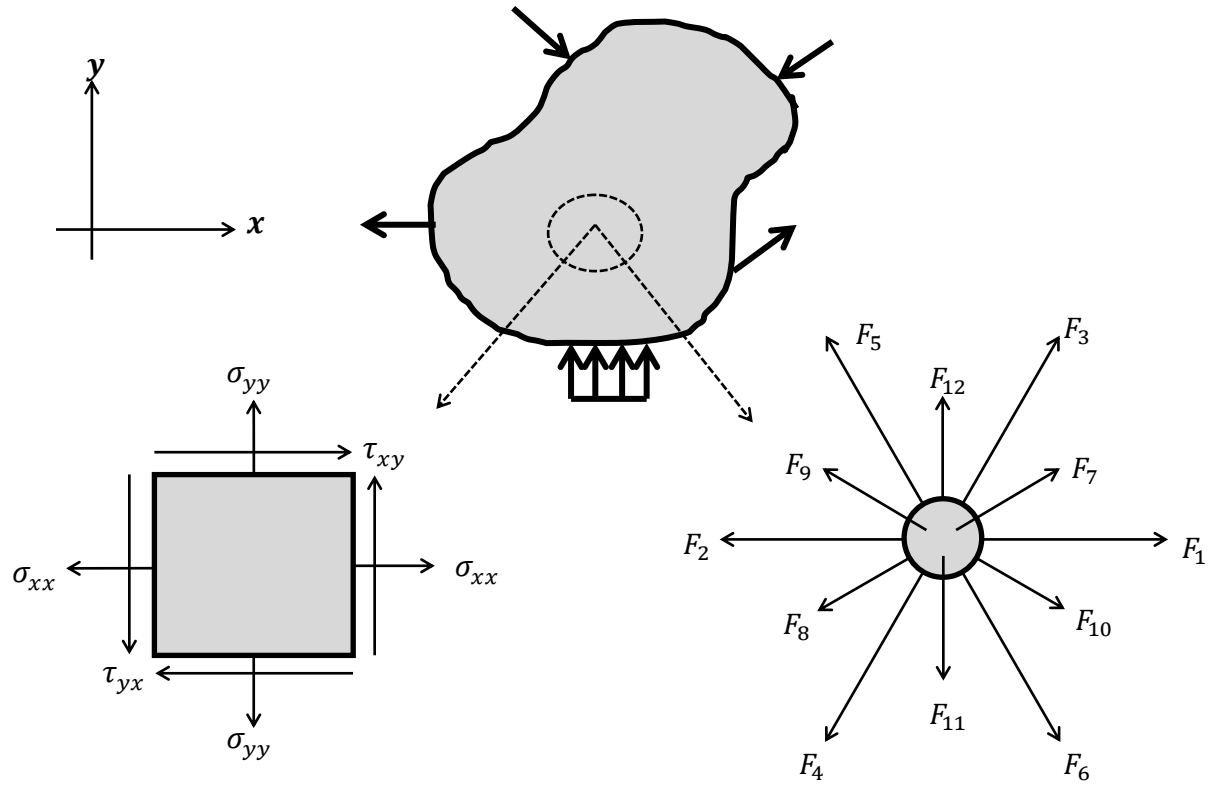

Figure 4.1 Classical Model vs. SPLM

$$\{\boldsymbol{\sigma}\} = \begin{Bmatrix} \sigma_{xx} \\ \sigma_{yy} \\ \tau_{xy} \\ \sigma_{zz} \\ \tau_{yz} \\ \tau_{zx} \end{Bmatrix} \tag{4.1}$$

and

$$\{\boldsymbol{T}\} = \begin{Bmatrix} F_1 \\ F_2 \\ \vdots \\ \vdots \\ F_{17} \\ F_{18} \end{Bmatrix}. \tag{4.2}$$

(Note that stress components in Equation 4.1 are organized differently from the traditional arrangement. The reason for this will be explained in Chapter 5.)

A comparison between the two models has an obvious challenge: How do we relate eighteen components of force to six components of stress? In general, the SPLM forces in collinear pd-bonds need not be equal to each other, e.g. $F_1 \neq F_2$. Under homogeneous conditions, translational symmetry considerations show that equal and opposite forces must exist in collinear pd-bonds.

Using the classical model for strain and assuming small deformations we define the six corresponding components of strain $\{\boldsymbol{\varepsilon}\}$: ε_{xx}, ε_{yy}, γ_{xy}, ε_{zz}, γ_{yz}, and γ_{zx}. Likewise, using the SPLM we define the corresponding pd-bond stretch state $\{\boldsymbol{S}\}$. In matrix form, the strain and the pd-bond stretch state are

$$\{\boldsymbol{\varepsilon}\} = \begin{Bmatrix} \varepsilon_{xx} \\ \varepsilon_{yy} \\ \gamma_{xy} \\ \varepsilon_{zz} \\ \gamma_{yz} \\ \gamma_{zx} \end{Bmatrix} \tag{4.3}$$

and

$$\{\boldsymbol{S}\} = \begin{Bmatrix} S_1 \\ S_2 \\ \vdots \\ \vdots \\ S_{17} \\ S_{18} \end{Bmatrix}. \tag{4.4}$$

Again, with the SPLM we know stretches in opposite collinear pd-bonds need not be equal to each other, e.g. $S_1 \neq S_2$. But for homogeneous conditions, translational symmetry considerations again require that the stretches in collinear pd-bonds will be equal.

We show in the remainder of this chapter that there are three key relationships that relate the classical model to SPLM when a spatially homogenous strain field exists. First, there is a relationship $[N]$ that will *expand* an equivalent pd-bond stretch state from the classical strain,

$$\{\boldsymbol{S}\} = [N]\{\boldsymbol{\varepsilon}\}. \tag{4.5}$$

Second, there is a relationship $[M]$ that will *reduce* the pd-bond force state to an equivalent classical stress,

$$\{\boldsymbol{\sigma}\} = [M]\{\boldsymbol{T}\}. \tag{4.6}$$

Finally, we will show that $[M]$ and $[N]$ are directly related to each other as follows:

$$[M] = \frac{1}{\sqrt{2}L^3}[N]^T[L_i]. \tag{4.7}$$

4.2 Virtual work-equivalence between SPLM and classical mechanics

We require virtual work-equivalent behavior under kinematically equivalent virtual deformations of both the classical mechanics model and the SPLM. Thus, when we have virtual deformation equivalence between the two models, the virtual work must also be equivalent,

$$\delta W_{Classical} = \delta W_{SPLM}\ . \tag{4.8}$$

The classical virtual work, $\delta W_{Classical}$, is equal to the stress times a virtual strain integrated over the volume,

$$\delta W_{Classical} = \lfloor\boldsymbol{\sigma}\rfloor\{\delta\boldsymbol{\varepsilon}\}\Delta V. \tag{4.9}$$

The SPLM virtual work, δW_{SPLM}, is equal to the sum of pd-bond forces times the pd-bond stretches integrated over half the pd-bond length,

$$\delta W_{SPLM} = \lfloor \boldsymbol{T} \rfloor \frac{[L_i]}{2} \{\delta \boldsymbol{S}\}, \tag{4.10}$$

where $[L_i]$ is the undeformed pd-bond length on the diagonal with zeros everywhere else,

$$[L_i] = \begin{bmatrix} L_1 & 0 & \cdots & 0 \\ 0 & L_2 & & \vdots \\ \vdots & & \ddots & 0 \\ 0 & \cdots & 0 & L_k \end{bmatrix}. \tag{4.11}$$

The reason that only one half of the pd-bond length is considered to find the internal work done in the particle is because each pd-bond is shared by two particles as shown in Figure 4.2. Plugging in Equation 4.9 and 4.10 into Equation 4.8 and simplifying yields

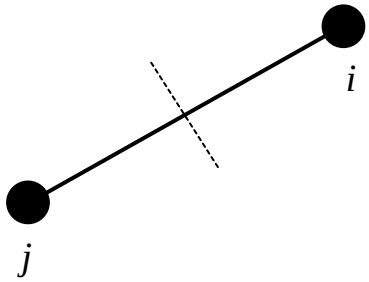

Figure 4.2, Shared pd-bond between two particles

$$\lfloor \boldsymbol{\sigma} \rfloor \{\delta \boldsymbol{\varepsilon}\} \Delta V = \frac{1}{2} \lfloor \boldsymbol{T} \rfloor [L_i] \{\delta \boldsymbol{S}\}. \tag{4.12}$$

We can substitute Equation 4.5 for $\{\delta \boldsymbol{S}\}$ and the transpose of Equation 4.6 for $\lfloor \boldsymbol{\sigma} \rfloor$ into Equation 4.12,

$$\lfloor \boldsymbol{T} \rfloor [M]^T \{\delta \boldsymbol{\varepsilon}\} \Delta V = \frac{1}{2} \lfloor \boldsymbol{T} \rfloor [L_i][N] \{\delta \boldsymbol{\varepsilon}\}. \tag{4.13}$$

For arbitrary $\lfloor \boldsymbol{T} \rfloor$ and $\{\delta \boldsymbol{\varepsilon}\}$, Equation 4.13 reduces to

$$[M]^T \Delta V = \frac{1}{2} [L_i][N]\,. \tag{4.14}$$

Recall from Chapter 3 that the tributary volume of a SPLM particle is

$$\Delta V = \frac{L^3}{\sqrt{2}}\,. \tag{3.1}$$

Taking the transpose of both sides as well as dividing both sides by ΔV, Equation 4.14 simplifies to Equation 4.7:

$$[M] = \frac{1}{\sqrt{2}L^3}[N]^T[L_i]. \tag{4.7}$$

Note that this equation is completely general for one, two, and three dimensional stress states and any type of lattice, even ones with non-collinear links.

4.3 The kinematic relationship between SPLM pd-bond stretch and classical strain

Consider a deformable body whose deformation can be represented by the classical infinitesimal strain tensor $[\boldsymbol{\varepsilon}]$, where

$$[\boldsymbol{\varepsilon}] = \begin{bmatrix} \varepsilon_{xx} & \gamma_{xy}/2 & \gamma_{xz}/2 \\ \gamma_{xy}/2 & \varepsilon_{yy} & \gamma_{yz}/2 \\ \gamma_{xz}/2 & \gamma_{yz}/2 & \varepsilon_{zz} \end{bmatrix}. \tag{4.15}$$

Now consider the pd-bond of original length L_i that is oriented in the direction shown in Figure 4.3. We can represent the unit direction vector, $\{\boldsymbol{n_i}\}$, of this pd-bond by the direction cosines,

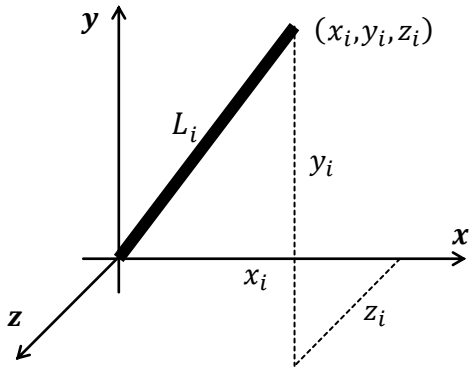

Figure 4.3, pd-bond unit elongation

$$\{\boldsymbol{n_i}\} = \begin{Bmatrix} n_{xi} \\ n_{yi} \\ n_{zi} \end{Bmatrix} = \begin{Bmatrix} x_i/L_i \\ y_i/L_i \\ z_i/L_i \end{Bmatrix}. \tag{4.16}$$

We now want to find the unit elongation, or the stretch S_i, of the pd-bond with respect to $[\boldsymbol{\varepsilon}]$. From the continuum mechanics infinitesimal deformation theory [6] the change in length per unit original length in the element in the $\{\boldsymbol{n_i}\}$ direction is

$$S_i = \lfloor \boldsymbol{n_i} \rfloor [\boldsymbol{\varepsilon}] \{\boldsymbol{n_i}\}. \tag{4.17}$$

Substituting Equation 4.15 and 4.16 into Equation 4.17 and performing the matrix operations yields,

$$S_i = \lfloor n_{xi} \quad n_{yi} \quad n_{zi} \rfloor \begin{bmatrix} \varepsilon_{xx} & \gamma_{xy}/2 & \gamma_{xz}/2 \\ \gamma_{xy}/2 & \varepsilon_{yy} & \gamma_{yz}/2 \\ \gamma_{xz}/2 & \gamma_{yz}/2 & \varepsilon_{zz} \end{bmatrix} \begin{Bmatrix} n_{xi} \\ n_{yi} \\ n_{zi} \end{Bmatrix},$$

$$S_i = {n_{xi}}^2 \varepsilon_{xx} + {n_{yi}}^2 \varepsilon_{yy} + {n_{zi}}^2 \varepsilon_{zz} + n_{xi} n_{yi} \gamma_{xy} + n_{yi} n_{zi} \gamma_{yz} + n_{zi} n_{xi} \gamma_{zx}. \tag{4.18}$$

Re-arranging terms, we then express Equation 4.18 in matrix form,

$$S_i = \begin{bmatrix} {n_{xi}}^2 & {n_{yi}}^2 & n_{xi} n_{yi} & {n_{zi}}^2 & n_{yi} n_{zi} & n_{zi} n_{xi} \end{bmatrix} \begin{Bmatrix} \varepsilon_{xx} \\ \varepsilon_{yy} \\ \gamma_{xy} \\ \varepsilon_{zz} \\ \gamma_{yz} \\ \gamma_{zx} \end{Bmatrix}. \tag{4.19}$$

Therefore, we can define $[N]$ as the matrix of direction cosines that map classical strains to SPLM stretches for all pd-bonds,

$$[N] = \begin{bmatrix} {n_{x1}}^2 & {n_{y1}}^2 & n_{x1} n_{y1} & {n_{z1}}^2 & n_{y1} n_{z1} & n_{z1} n_{x1} \\ {n_{x2}}^2 & {n_{y2}}^2 & n_{x2} n_{y2} & {n_{z2}}^2 & n_{y2} n_{z2} & n_{z2} n_{x2} \\ \vdots & \vdots & \vdots & \vdots & \vdots & \vdots \\ {n_{xi}}^2 & {n_{yi}}^2 & n_{xi} n_{yi} & {n_{zi}}^2 & n_{yi} n_{zi} & n_{zi} n_{xi} \end{bmatrix}. \tag{4.20}$$

4.4 The relationship between SPLM and classical mechanics for a 3D HCP lattice

Consider the three-dimensional SPLM particle shown in Figure 3.2. We assume the state of a three-dimensional particle is a function of its twelve nearest neighbors and six second-nearest neighbors (the reason for including second-nearest neighbors will be explained in Chapter 5). We now solve the $[N]$ matrix for when particles are arranged by a HCP lattice.

Using Table 3.1 from Chapter 3, we solve for the direction cosines of each pd-bond, using Matlab, yielding

$$[N] = \begin{bmatrix} 1 & 0 & 0 & 0 & 0 & 0 \\ 1 & 0 & 0 & 0 & 0 & 0 \\ 1/4 & 3/4 & \sqrt{3}/4 & 0 & 0 & 0 \\ 1/4 & 3/4 & \sqrt{3}/4 & 0 & 0 & 0 \\ 1/4 & 3/4 & -\sqrt{3}/4 & 0 & 0 & 0 \\ 1/4 & 3/4 & -\sqrt{3}/4 & 0 & 0 & 0 \\ 1/4 & 1/12 & \sqrt{3}/12 & 2/3 & \sqrt{2}/6 & \sqrt{6}/6 \\ 1/4 & 1/12 & \sqrt{3}/12 & 2/3 & \sqrt{2}/6 & \sqrt{6}/6 \\ 1/4 & 1/12 & -\sqrt{3}/12 & 2/3 & \sqrt{2}/6 & -\sqrt{6}/6 \\ 1/4 & 1/12 & -\sqrt{3}/12 & 2/3 & \sqrt{2}/6 & -\sqrt{6}/6 \\ 0 & 1/3 & 0 & 2/3 & -\sqrt{2}/3 & 0 \\ 0 & 1/3 & 0 & 2/3 & -\sqrt{2}/3 & 0 \\ 1/2 & 1/6 & \sqrt{3}/6 & 1/3 & -\sqrt{2}/6 & -\sqrt{6}/6 \\ 1/2 & 1/6 & \sqrt{3}/6 & 1/3 & -\sqrt{2}/6 & -\sqrt{6}/6 \\ 0 & 2/3 & 0 & 1/3 & \sqrt{2}/3 & 0 \\ 0 & 2/3 & 0 & 1/3 & \sqrt{2}/3 & 0 \\ 1/2 & 1/6 & -\sqrt{3}/6 & 1/3 & -\sqrt{2}/6 & \sqrt{6}/6 \\ 1/2 & 1/6 & -\sqrt{3}/6 & 1/3 & -\sqrt{2}/6 & \sqrt{6}/6 \end{bmatrix}. \tag{4.21}$$

The pd-bond length matrix $[L_i]$ of a three-dimensional particle contains two different lengths, L for the twelve nearest neighbors and $\sqrt{2}L$ for the six second nearest neighbors,

$$[L_i] = \begin{bmatrix} \underset{(12\times 12)}{\begin{bmatrix} L & 0 & \cdots & 0 \\ 0 & L & & \vdots \\ \vdots & & \ddots & 0 \\ 0 & \cdots & 0 & L \end{bmatrix}} & \underset{(12\times 6)}{[0]} \\ \underset{(6\times 12)}{[0]} & \underset{(6\times 6)}{\begin{bmatrix} \sqrt{2}L & 0 & \cdots & 0 \\ 0 & \sqrt{2}L & & \vdots \\ \vdots & & \ddots & 0 \\ 0 & \cdots & 0 & \sqrt{2}L \end{bmatrix}} \end{bmatrix}. \tag{4.22}$$

Substituting Equations 4.21 and 4.22 into Equation 4.7, we now solve for $[M]$ for the three-dimensional case. Using Matlab,

$$[M] = \frac{1}{L^2}\begin{bmatrix} \frac{\sqrt{2}}{2} & \frac{\sqrt{2}}{2} & \frac{\sqrt{2}}{8} & \frac{\sqrt{2}}{8} & \frac{\sqrt{2}}{8} & \frac{\sqrt{2}}{8} & \frac{\sqrt{2}}{8} & \frac{\sqrt{2}}{8} & \frac{\sqrt{2}}{8} & \cdots \\ 0 & 0 & \frac{3\sqrt{2}}{8} & \frac{3\sqrt{2}}{8} & \frac{3\sqrt{2}}{8} & \frac{3\sqrt{2}}{8} & \frac{\sqrt{2}}{24} & \frac{\sqrt{2}}{24} & \frac{\sqrt{2}}{24} & \cdots \\ 0 & 0 & \frac{\sqrt{6}}{8} & \frac{\sqrt{6}}{8} & -\frac{\sqrt{6}}{8} & -\frac{\sqrt{6}}{8} & \frac{\sqrt{6}}{24} & \frac{\sqrt{6}}{24} & -\frac{\sqrt{6}}{24} & \cdots \\ 0 & 0 & 0 & 0 & 0 & 0 & \frac{\sqrt{2}}{3} & \frac{\sqrt{2}}{3} & \frac{\sqrt{2}}{3} & \cdots \\ 0 & 0 & 0 & 0 & 0 & 0 & \frac{1}{6} & \frac{1}{6} & \frac{1}{6} & \cdots \\ 0 & 0 & 0 & 0 & 0 & 0 & \frac{\sqrt{3}}{6} & \frac{\sqrt{3}}{6} & -\frac{\sqrt{3}}{6} & \cdots \end{bmatrix}$$

$$\begin{bmatrix} \cdots & \frac{\sqrt{2}}{8} & 0 & 0 & \frac{1}{2} & \frac{1}{2} & 0 & 0 & \frac{1}{2} & \frac{1}{2} \\ \cdots & \frac{\sqrt{2}}{24} & \frac{\sqrt{2}}{6} & \frac{\sqrt{2}}{6} & \frac{1}{6} & \frac{1}{6} & \frac{2}{3} & \frac{2}{3} & \frac{1}{6} & \frac{1}{6} \\ \cdots & -\frac{\sqrt{6}}{24} & 0 & 0 & \frac{\sqrt{3}}{6} & \frac{\sqrt{3}}{6} & 0 & 0 & -\frac{\sqrt{3}}{6} & -\frac{\sqrt{3}}{6} \\ \cdots & \frac{\sqrt{2}}{3} & \frac{\sqrt{2}}{3} & \frac{\sqrt{2}}{3} & \frac{1}{3} & \frac{1}{3} & \frac{1}{3} & \frac{1}{3} & \frac{1}{3} & \frac{1}{3} \\ \cdots & \frac{1}{6} & -\frac{1}{3} & -\frac{1}{3} & -\frac{\sqrt{2}}{6} & -\frac{\sqrt{2}}{6} & \frac{\sqrt{2}}{3} & \frac{\sqrt{2}}{3} & -\frac{\sqrt{2}}{6} & -\frac{\sqrt{2}}{6} \\ \cdots & -\frac{\sqrt{3}}{6} & 0 & 0 & -\frac{\sqrt{6}}{6} & -\frac{\sqrt{6}}{6} & 0 & 0 & \frac{\sqrt{6}}{6} & \frac{\sqrt{6}}{6} \end{bmatrix} \quad (4.23)$$

4.5 Summary

In this chapter we have defined the relationship between SPLM and classical mechanics for the full three-dimensional case. Again, these relationships are only valid under a spatially homogenous and infinitesimal strain field. When these conditions are met, we have shown that the classical strain can be expanded to the SPLM pd-bond stretch state using the direction cosine matrix $[N]$. By assuming strain energy equivalence between the two models we have shown the relationship between $[M]$ and $[N]$. From $[M]$, the classical stress can be reduced from the SPLM pd-bond force state. The relationships developed in this chapter are completely independent of any constitutive model. This brings us to our next chapter which defines the SPLM constitutive relationship between the pd-bond force state and the pd-bond stretch state.

Chapter 5

SPLM Linear Elasticity

5.1 Introduction

In this chapter we define the SPLM constitutive linear-elastic relationship $[K]$ between the pd-bond force state $\{\boldsymbol{T}\}$ and the elastic pd-bond stretch state $\{\boldsymbol{S^e}\}$. Assuming that the particles are arranged in a hexagonal close packed (HCP) lattice, we will define $[K]$ for the three-dimensional case. We will then define SPLM linear elasticity for the uniaxial one-dimensional, two-dimensional plane stress, and two-dimensional plane strain special cases.

We must first clearly state that, perhaps surprisingly, there is not just one unique constitutive relationship between pd-bond force state and pd-bond stretch state. There are an infinite number of possible micro-elastic constitutive solutions that will ensure isotropy and identical macro-elastic behavior regardless of lattice orientation. However, for any solution, we require that when there exists a spatially homogeneous strain field and infinitesimal deformations that the corresponding SPLM constitutive relationship $[K]$ be work-equivalent under all deformations to the classical mechanics constitutive relationship $[D]$. Thus, we will first define the relationship between $[K]$ and $[D]$ for situations where a comparison can be made.

5.2 The relationship between SPLM and classical constitutive models

We assume that there exists a spatially homogeneous strain field and deformations are small. For a given particle, we assert that the pd-bond force state $\{\boldsymbol{T}\}$ is a linear function the elastic pd-bond stretch state $\{\boldsymbol{S^e}\}$ via the symmetric constitutive matrix $[K]$,

$$\{\boldsymbol{T}\} = [K]\{\boldsymbol{S^e}\}. \tag{5.1}$$

From linear elastic mechanics, we know that the stress $\{\boldsymbol{\sigma}\}$ is related to the elastic strain $\{\boldsymbol{\varepsilon}^{\boldsymbol{e}}\}$ by the symmetric constitutive matrix $[D]$,

$$\{\boldsymbol{\sigma}\} = [D]\{\boldsymbol{\varepsilon}^{\boldsymbol{e}}\}. \tag{5.2}$$

Recall from Chapter 4 that we can expand a pd-bond stretch state from the general infinitesimal strain using the matrix $[N]$,

$$\{\boldsymbol{S}\} = [N]\{\boldsymbol{\varepsilon}\}, \tag{4.5}$$

and that $[N]$ and $[M]$ ($\{\boldsymbol{\sigma}\} = [M]\{\boldsymbol{T}\}$ is the relationship that reduces a pd-bond force state to an equivalent stress) are related by

$$[M] = \frac{1}{\sqrt{2}L^3}[N]^T[L_i], \tag{4.7}$$

where $[L_i]$ square diagonal matrix that contains the undeformed pd-bond lengths. Because $[N]$ is strictly a kinematic relationship, it is also valid for expanding the elastic pd-bond stretch state from the elastic strain,

$$\{\boldsymbol{S}^{\boldsymbol{e}}\} = [N]\{\boldsymbol{\varepsilon}^{\boldsymbol{e}}\}. \tag{5.3}$$

We require that when we have deformation equivalence between the two models that the virtual work done on a particle must also be equivalent. As shown in Chapter 4:

$$\delta W_{Classical} = \delta W_{SPLM} \ . \tag{4.8}$$

or

$$\lfloor \boldsymbol{\sigma} \rfloor \{\delta \boldsymbol{\varepsilon}^{\boldsymbol{e}}\} \Delta V = \frac{1}{2}\lfloor \boldsymbol{T} \rfloor [L_i]\{\delta \boldsymbol{S}^{\boldsymbol{e}}\}. \tag{4.12}$$

Note that we have substituted in virtual elastic strains and virtual elastic pd-bond stretch states. However, as shown in chapter 4, this deformation equivalence relationship is valid regardless of elasticity. We then substitute the transpose of Equation 5.1 and the transpose of Equation 5.2 into Equation 4.12,

$$\lfloor \delta \boldsymbol{\varepsilon}^{\boldsymbol{e}} \rfloor [D] \{ \delta \boldsymbol{\varepsilon}^{\boldsymbol{e}} \} \Delta V = \frac{1}{2} \lfloor \delta \boldsymbol{S}^{\boldsymbol{e}} \rfloor [K] [L_i] \{ \delta \boldsymbol{S}^{\boldsymbol{e}} \}. \tag{5.4}$$

Using Equation 5.3, we can represent the virtual elastic pd-bond stretch state in terms of the virtual elastic strains,

$$\lfloor \delta \boldsymbol{\varepsilon}^{\boldsymbol{e}} \rfloor [D] \{ \delta \boldsymbol{\varepsilon}^{\boldsymbol{e}} \} \Delta V = \frac{1}{2} \lfloor \delta \boldsymbol{\varepsilon}^{\boldsymbol{e}} \rfloor [N]^T [K] [L_i] [N] \{ \delta \boldsymbol{\varepsilon}^{\boldsymbol{e}} \}. \tag{5.5}$$

For arbitrary virtual elastic strains and recalling that the tributary volume of a SPLM particle is $\Delta V = \frac{L^3}{\sqrt{2}}$., Equation 5.5 reduces to

$$[D] = \frac{1}{\sqrt{2} L^3} [N]^T [K] [L_i] [N]. \tag{5.6}$$

We can rearrange Equation 4.7 to solve for $[N]^T$,

$$[N]^T = \left(\sqrt{2} L^3 \right) [M] [L_i]^{-1}, \tag{5.7}$$

and then substitute Equation 5.7 into Equation 5.6,

$$[D] = \frac{1}{\sqrt{2} L^3} \left(\sqrt{2} L^3 \right) [M] [L_i]^{-1} [K] [L_i] [N]. \tag{5.8}$$

Because $[K]$ is symmetric, $[L_i]^{-1} [K] [L_i] = [K]$. Simplifying Equation 5.8 yields

$$[D] = [M] [K] [N]. \tag{5.9}$$

We cannot solve for $[K]$ directly because $[N]$ and $[M]$ are not square matrixes; however we can assume a solution for $[K]$ in terms of symbolic variables. We then compare the matrix produced by evaluating $[M][K][N]$ and the classical constitutive matrix $[D]$ to solve for the variables. We now define one possible solution for $[K]$ for the general three-dimensional case.

5.3 SPLM constitutive model for 3D HCP lattice

We assume that a three dimensional particle interacts with its twelve nearest neighbors as well as its six second-nearest neighbors. Originally we considered only the nearest neighbors; however we soon discovered that this was insufficient to guarantee isotropy for all values of Poisson's ratio. Therefore, we assume that a three-dimensional particle interacts also with its second-nearest neighbors. For the twelve first nearest neighboring pd-bonds, of length L, we assume that pd-bond force state, $(F_i)_{1^{st}}$, is equal to the elastic pd-bond stretch state, $(S_i{}^e)_{1^{st}}$, multiplied by the constant a plus the average elastic pd-bond stretch state of all twelve nearest neighbors, $(S_{AVG}{}^e)_{1^{st}}$, multiplied by the constant b,

$$(F_i)_{1^{st}} = a(S_i{}^e)_{1^{st}} + b(S_{AVG}{}^e)_{1^{st}} \tag{5.10}$$

where

$$(S_{AVG}{}^e)_{1^{st}} = \frac{1}{12}\sum_{i=1}^{12}(S_i{}^e)_{1^{st}}. \tag{5.11}$$

For the six second-nearest neighboring links, of length $\sqrt{2}L$, we assume that pd-bond force state, $(F_i)_{2^{nd}}$, is equal to the elastic pd-bond stretch state, $(S_i{}^e)_{2^{nd}}$, multiplied by the constant c,

$$(F_i)_{2^{nd}} = c(S_i{}^e)_{2^{nd}}. \tag{5.12}$$

From Equations 5.10, 5.11, and 5.12 we produce a symmetric $[K]$ matrix,

$$[K] = \begin{matrix} (12\times 12) \\ \\ \\ \\ \\ \\ (6\times 12) \end{matrix} \begin{matrix} \left[\begin{matrix} a+\frac{b}{12} & \frac{b}{12} & \frac{b}{12} & \cdots & \cdots & \frac{b}{12} \\ \frac{b}{12} & a+\frac{b}{12} & \frac{b}{12} & \cdots & \cdots & \frac{b}{12} \\ \vdots & \vdots & & \ddots & & \vdots \\ \vdots & \vdots & & & \ddots & \frac{b}{12} \\ \frac{b}{12} & \frac{b}{12} & \cdots & \cdots & \frac{b}{12} & a+\frac{b}{12} \end{matrix}\right. \\ \\ \left[0\right] \end{matrix} \begin{matrix} (12\times 6) \\ \left[0\right] \\ \\ \left[\begin{matrix} c & 0 & \cdots & 0 \\ 0 & c & & \vdots \\ \vdots & & \ddots & 0 \\ 0 & \cdots & 0 & c \end{matrix}\right] \\ (6\times 6) \end{matrix} \quad (5.13)$$

where the last six rows represent the second-nearest neighbors. In three-dimensions, the classical mechanics constitutive matrix $[D]$ is

$$[D] = \frac{E}{(1+\nu)(1-2\nu)} \begin{bmatrix} (1-\nu) & \nu & 0 & \nu & 0 & 0 \\ \nu & (1-\nu) & 0 & \nu & 0 & 0 \\ 0 & 0 & \frac{(1-2\nu)}{2} & 0 & 0 & 0 \\ \nu & \nu & 0 & (1-\nu) & 0 & 0 \\ 0 & 0 & 0 & 0 & \frac{(1-2\nu)}{2} & 0 \\ 0 & 0 & 0 & 0 & 0 & \frac{(1-2\nu)}{2} \end{bmatrix}. \quad (5.14)$$

Note that $[D]$ has been rearranged to be consistent with the stress and strain defined in Chapter 4. Using $[N]$ and $[M]$ defined in Chapter 4 for a three dimensional particle, we substitute in Equations 4.25, 4.27, 5.13, and 5.14 into Equation 5.9 and reduce:

$$\frac{E}{(1+\nu)(1-2\nu)} \begin{bmatrix} (1-\nu) & \nu & 0 & \nu & 0 & 0 \\ \nu & (1-\nu) & 0 & \nu & 0 & 0 \\ 0 & 0 & \frac{(1-2\nu)}{2} & 0 & 0 & 0 \\ \nu & \nu & 0 & (1-\nu) & 0 & 0 \\ 0 & 0 & 0 & 0 & \frac{(1-2\nu)}{2} & 0 \\ 0 & 0 & 0 & 0 & 0 & \frac{(1-2\nu)}{2} \end{bmatrix} = \cdots$$

$$\frac{\sqrt{2}}{L^2}\begin{bmatrix} \left(\frac{5a}{4}+\frac{2b}{3}+\frac{c}{\sqrt{2}}\right) & \left(\frac{5a}{12}+\frac{2b}{3}+\frac{\sqrt{2}c}{12}\right) & 0 & \left(\frac{a}{3}+\frac{2b}{3}+\frac{\sqrt{2}c}{3}\right) & \left(\frac{\sqrt{2}a}{12}-\frac{c}{3}\right) & 0 \\ \left(\frac{5a}{12}+\frac{2b}{3}+\frac{\sqrt{2}c}{12}\right) & \left(\frac{5a}{4}+\frac{2b}{3}+\frac{\sqrt{2}c}{2}\right) & 0 & \left(\frac{a}{3}+\frac{2b}{3}+\frac{\sqrt{2}c}{3}\right) & \left(-\frac{\sqrt{2}a}{12}+\frac{c}{3}\right) & 0 \\ 0 & 0 & \left(\frac{5a}{12}+\frac{\sqrt{2}c}{6}\right) & 0 & 0 & \left(\frac{\sqrt{2}a}{12}-\frac{c}{3}\right) \\ \left(\frac{a}{3}+\frac{2b}{3}+\frac{\sqrt{2}c}{3}\right) & \left(\frac{a}{3}+\frac{2b}{3}+\frac{\sqrt{2}c}{3}\right) & 0 & \left(\frac{4a}{3}+\frac{2b}{3}+\frac{\sqrt{2}c}{3}\right) & 0 & 0 \\ \left(\frac{\sqrt{2}a}{12}-\frac{c}{3}\right) & \left(-\frac{\sqrt{2}a}{12}+\frac{c}{3}\right) & 0 & 0 & \left(\frac{a}{3}+\frac{\sqrt{2}c}{3}\right) & 0 \\ 0 & 0 & 0 & \left(\frac{\sqrt{2}a}{12}-\frac{c}{3}\right) & 0 & \left(\frac{a}{3}+\frac{\sqrt{2}c}{3}\right) \end{bmatrix}$$

(5.15)

We then set corresponding elements equal to each other (i.e. $D_{11} = (MKN)_{11}$) from Equation 5.15; this produces three linear equations with three unknowns, a, b, and c. Using the Matlab symbolic toolkit (see Appendix), we solve for a, b, and c:

$$a = \frac{1}{\sqrt{2}} \cdot \frac{EL^2}{(v+1)} \tag{5.15}$$

$$b = \frac{3\sqrt{2}}{8} \cdot \frac{E\,L^2\,(1-4v)}{(2v-1)(v+1)} \tag{5.16}$$

$$c = \frac{1}{4} \cdot \frac{EL^2}{(v+1)} = \frac{1}{2\sqrt{2}}a \tag{5.17}$$

Therefore, plugging these constants back into Equation 5.13 provides one possible constitutive relationship $[K]$ between three dimensional pd-bond force state and elastic pd-bond stretch state that will ensure isotropy for different values of Poisson's ratio.

5.4 Reducing the pd-bond stretch state to strain for special cases

Thus far we have defined SPLM for the fully three-dimensional cases. However SPLM can be adapted to model uniaxial one-dimensional, two-dimensional plane stress, and two-

dimensional plane strain special cases. In all of these cases, a SPLM particle still has eighteen pd-bonds but only the in-axis or in-plane pd-bond stretches are computed. Therefore we must define a method that will calculate all eighteen pd-bond stretches from the computed in-axis or in-plane stretches. This method will require that a simplified (in-axis or in-plane stretches only) pd-bond stretch state, $\{\boldsymbol{S}'\}$, be reduced to an equivalent classical strain,

$$\{\boldsymbol{\varepsilon}\} = [N']\{\boldsymbol{S}'\}, \tag{5.18}$$

where $[N']$ is the simplified reduction matrix.

Recall from chapter 4 that a comparison between SPLM and classical mechanics can only be made where there exists a spatially homogeneous strain field thus the stretches in collinear pd-bonds must be equal, i.e. $S_1 = S_2$. Therefore (for special cases) we average the pd-bond stretch state $\{\boldsymbol{S}\}$ to the average pd-bond stretch state $\{\overline{\boldsymbol{S}}\}$,

$$\{\overline{\boldsymbol{S}}\} = \begin{Bmatrix} \frac{S_1+S_2}{2} \\ \frac{S_3+S_4}{2} \\ \vdots \\ \frac{S_i+S_{i+1}}{2} \end{Bmatrix}. \tag{5.19}$$

We then define a square matrix $[\overline{N}]$ that expands the average pd-bond stretch state $\{\overline{\boldsymbol{S}}\}$ from the classical strain,

$$\{\overline{\boldsymbol{S}}\} = [\overline{N}]\{\boldsymbol{\varepsilon}\}. \tag{5.20}$$

Now that $[\overline{N}]$ is a square matrix, we can pre-multiply both sides of Equation 5.20 by $[\overline{N}]^{-1}$ and thus reduce the average pd-bond stretch state to the equivalent classical strain,

$$\{\boldsymbol{\varepsilon}\} = [\overline{N}]^{-1}\{\overline{\boldsymbol{S}}\}. \tag{5.21}$$

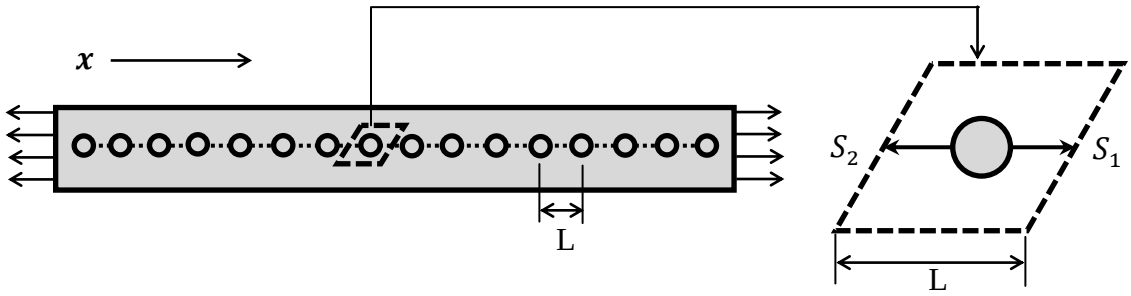

Figure 5.1 1D lattice strand with in-axis particle pd-bond stretches

We first consider the one-dimensional case represented by a strand of particles with in-axis stretches S_1 and S_2 (shown in figure 5.1). For one-dimensional problems the simplified pd-bond stretch state is the two in-axis pd-bond stretches,

$$\{\boldsymbol{S}'\} = \begin{Bmatrix} S_1 \\ S_2 \end{Bmatrix}. \tag{5.22}$$

We can then average the simplified the in-axis pd-bond stretch state $\{\boldsymbol{S}'\}$ to the average in-axis pd-bond stretch state $\{\overline{\boldsymbol{S}}\}$,

$$\{\overline{\boldsymbol{S}}\} = \left\{\frac{S_1+S_2}{2}\right\} = \frac{1}{2}[1 \quad 1]\begin{Bmatrix} S_1 \\ S_2 \end{Bmatrix}. \tag{5.23}$$

From Table 3.1 we solve for $[N]$ for the simplified one dimensional case as follows:

$$[N] = \begin{bmatrix} {n_{x1}}^2 \\ {n_{x2}}^2 \end{bmatrix} = \begin{bmatrix} (L/L)^2 \\ (-L/L)^2 \end{bmatrix},$$

$$[N] = \begin{bmatrix} 1 \\ 1 \end{bmatrix}. \tag{5.24}$$

Matrix rows one and two are both the same in Equation 5.24, therefore we can simplify $[N]$ to

$$[\overline{N}] = [1] = 1. \tag{5.25}$$

The classical one-dimensional case the strain is

$$\{\boldsymbol{\varepsilon}\} = \{\varepsilon_{xx}\}. \tag{5.26}$$

Substituting Equations 5.23, 5.25, and 5.26 into Equation 5.20 yields

$$\tfrac{1}{2}[1 \quad 1]\begin{Bmatrix} S_1 \\ S_2 \end{Bmatrix} = 1 \cdot \{\varepsilon_{xx}\}. \tag{5.27}$$

Rearranging Equation 5.27 yields the relationship that will reduce the simplified pd-bond stretch state to the classical strain for the one-dimensional case,

$$\{\varepsilon_{xx}\} = \tfrac{1}{2}[1 \quad 1]\begin{Bmatrix} S_1 \\ S_2 \end{Bmatrix}, \tag{5.27}$$

where the reduction matrix $[N']$ is

$$[N'] = \tfrac{1}{2}[1 \quad 1]. \tag{5.28}$$

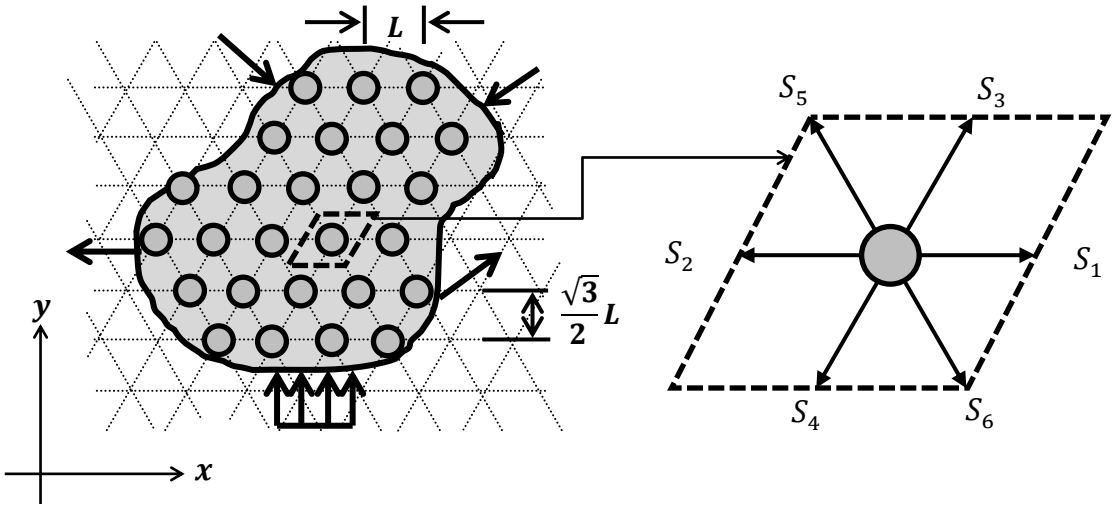

Figure 5.2 2D lattice plane with in-plane particle pd-bond stretches

Next we consider the two-dimensional case represented by a layer of particles with in-plane stretches S_1, S_2, S_3, S_4, S_5, and S_6 (shown in figure 5.2). For two-dimensional problems, the simplified pd-bond stretch state is the six in-plane pd-bond stretches,

$$\{\boldsymbol{S}'\} = \begin{Bmatrix} S_1 \\ S_2 \\ S_3 \\ S_4 \\ S_5 \\ S_6 \end{Bmatrix}. \tag{5.29}$$

We then average the simplified in-plane pd-bond stretch state $\{\boldsymbol{S}'\}$ to the average in-plane pd-bond stretch state $\{\overline{\boldsymbol{S}}\}$,

$$\{\overline{\boldsymbol{S}}\} = \begin{Bmatrix} \frac{S_1+S_2}{2} \\ \frac{S_3+S_4}{2} \\ \frac{S_5+S_6}{2} \end{Bmatrix} = \frac{1}{2}\begin{bmatrix} 1 & 1 & 0 & 0 & 0 & 0 \\ 0 & 0 & 1 & 1 & 0 & 0 \\ 0 & 0 & 0 & 0 & 1 & 1 \end{bmatrix} \begin{Bmatrix} S_1 \\ S_2 \\ S_3 \\ S_4 \\ S_5 \\ S_6 \end{Bmatrix}. \tag{5.30}$$

Considering only the in plane links, using Table 3.1 the $[N]$ for the simplified two-dimensional case is as follows:

$$[N] = \begin{bmatrix} {n_{x1}}^2 & {n_{y1}}^2 & n_{x1}n_{y1} \\ \vdots & \vdots & \vdots \\ {n_{x6}}^2 & {n_{y6}}^2 & n_{x6}n_{y6} \end{bmatrix} = \begin{bmatrix} \left(\frac{L}{L}\right)^2 & \left(\frac{0}{L}\right)^2 & \left(\frac{L}{L}\right)\left(\frac{0}{L}\right) \\ \left(\frac{-L}{L}\right)^2 & \left(\frac{0}{L}\right)^2 & \left(\frac{-L}{L}\right)\left(\frac{0}{L}\right) \\ \left(\frac{L/2}{L}\right)^2 & \left(\frac{L\sqrt{3}/2}{L}\right)^2 & \left(\frac{L/2}{L}\right)\left(\frac{L\sqrt{3}/2}{L}\right) \\ \left(\frac{-L/2}{L}\right)^2 & \left(\frac{-L\sqrt{3}/2}{L}\right)^2 & \left(\frac{-L/2}{L}\right)\left(\frac{-L\sqrt{3}/2}{L}\right) \\ \left(\frac{-L/2}{L}\right)^2 & \left(\frac{L\sqrt{3}/2}{L}\right)^2 & \left(\frac{-L/2}{L}\right)\left(\frac{L\sqrt{3}/2}{L}\right) \\ \left(\frac{L/2}{L}\right)^2 & \left(\frac{-L\sqrt{3}/2}{L}\right)^2 & \left(\frac{L/2}{L}\right)\left(\frac{-L\sqrt{3}/2}{L}\right) \end{bmatrix},$$

$$[N] = \begin{bmatrix} 1 & 0 & 0 \\ 1 & 0 & 0 \\ 1/4 & 3/4 & \sqrt{3}/4 \\ 1/4 & 3/4 & \sqrt{3}/4 \\ 1/4 & 3/4 & -\sqrt{3}/4 \\ 1/4 & 3/4 & -\sqrt{3}/4 \end{bmatrix}. \tag{5.31}$$

We can see in Equation 5.31 that rows one and two, rows three and four, and rows five and six are the same. Therefore, we can simplify $[N]$ to $[\bar{N}]$:

$$[\bar{N}] = \begin{bmatrix} 1 & 0 & 0 \\ 1/4 & 3/4 & \sqrt{3}/4 \\ 1/4 & 3/4 & -\sqrt{3}/4 \end{bmatrix}. \tag{5.32}$$

Taking the inverse of Equation 5.32 yields,

$$[\bar{N}]^{-1} = \begin{bmatrix} 1 & 0 & 0 \\ -1/3 & 2/3 & 2/3 \\ 0 & 2/\sqrt{3} & -2/\sqrt{3} \end{bmatrix}. \tag{5.33}$$

The classical two-dimensional strains are

$$\{\boldsymbol{\varepsilon}\} = \begin{Bmatrix} \varepsilon_{xx} \\ \varepsilon_{yy} \\ \gamma_{xy} \end{Bmatrix}. \tag{5.34}$$

Substituting Equations 5.30, 5.33, and 5.34 into Equation 5.21 yields

$$\begin{Bmatrix} \varepsilon_{xx} \\ \varepsilon_{yy} \\ \gamma_{xy} \end{Bmatrix} = \begin{bmatrix} 1 & 0 & 0 \\ -1/3 & 2/3 & 2/3 \\ 0 & 2/\sqrt{3} & -2/\sqrt{3} \end{bmatrix} \cdot \frac{1}{2} \begin{bmatrix} 1 & 1 & 0 & 0 & 0 & 0 \\ 0 & 0 & 1 & 1 & 0 & 0 \\ 0 & 0 & 0 & 0 & 1 & 1 \end{bmatrix} \begin{Bmatrix} S_1 \\ S_2 \\ S_3 \\ S_4 \\ S_5 \\ S_6 \end{Bmatrix},$$

$$\begin{Bmatrix}\varepsilon_{xx}\\ \varepsilon_{yy}\\ \gamma_{xy}\end{Bmatrix}=\begin{bmatrix}1/2 & 1/2 & 0 & 0 & 0 & 0\\ -1/6 & -1/6 & 1/3 & 1/3 & 1/3 & 1/3\\ 0 & 0 & 1/\sqrt{3} & 1/\sqrt{3} & -1/\sqrt{3} & -1/\sqrt{3}\end{bmatrix}\begin{Bmatrix}S_1\\ S_2\\ S_3\\ S_4\\ S_5\\ S_6\end{Bmatrix}. \quad (5.35)$$

Therefore, the $[N']$ that will reduce the simplified in-plane pd-bond stretch state to the classical strain for the two-dimensional is

$$[N']=\begin{bmatrix}1/2 & 1/2 & 0 & 0 & 0 & 0\\ -1/6 & -1/6 & 1/3 & 1/3 & 1/3 & 1/3\\ 0 & 0 & 1/\sqrt{3} & 1/\sqrt{3} & -1/\sqrt{3} & -1/\sqrt{3}\end{bmatrix}. \quad (5.36)$$

This method can be used to reduce a simplified stretch state an equivalent classical strain for one- and two-dimensional problems, assuming that the particle is not at a boundary. If the particle does happen to be at a boundary, as shown in Figure 5.3, one or more of the pd-bond stretches may not be calculated because there is not a neighboring particle. In this case we assume that the stretch of the pd-bond at a boundary is equal to the stretch of its collinear pd-bond, i.e. $S_2 = S_1$. Thus, we can still reduce the stretch state of a boundary particle to an equivalent strain.

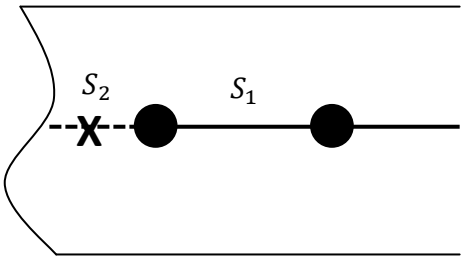

Figure 5.3, SPLM particle at a boundary

5.5 SPLM stretch state for 1D uniaxial lattice strand

Consider a bar with a prismatic cross-section and is un-constrained in the out-of-axis direction. Under these conditions, the SPLM three-dimensional model can be simplified to a one-dimensional lattice strand of particles. The cross-sectional area of this lattice strand is the tributary area of a SPLM particle, $A_{STRAND} = \frac{L^2}{\sqrt{2}}$. Therefore the uniaxial force carried by the

strand of particles, F_{STRAND}, is proportional to the uniaxial force carried by the bar, F_{BAR}, with respect to the bar's cross-sectional area, A_{BAR},

$$F_{STRAND} = F_{BAR}\left(\frac{A_{STRAND}}{A_{BAR}}\right). \tag{5.37}$$

A SPLM particle in a lattice strand still had eighteen pd-bonds in and out of axis with the strand. The stretch of pd-bonds in the out of axis directions are non-zero and, while the net forces on the particle in the out-of-axis directions are zero, the pd-bonds in the out-of-axis directions do have forces in them. To fully define the particle elastic stretch state $\{\boldsymbol{S}^{\boldsymbol{e}}\}$ for the one-dimensional uniaxial special case, we must first show that the elastic stretch state of all eighteen pd-bonds is a function the two in-axis elastic pd-bonds stretches,

$$\{\boldsymbol{S}^{\boldsymbol{e}}\} = [C]\{\boldsymbol{S'}^{\boldsymbol{e}}\}. \tag{5.38}$$

where $[C]$ converts the simplified elastic stretch state to the full elastic stretch state. We begin by recalling the classical mechanics constitutive relationship, Equation 5.2,

$$\{\boldsymbol{\sigma}\} = [D]\{\boldsymbol{\varepsilon}^{\boldsymbol{e}}\}. \tag{5.2}$$

In classical mechanics, the stress and strain of a bar subjected to uniaxial stress are

$$\{\boldsymbol{\sigma}\} = \begin{Bmatrix} \sigma_{xx} \\ 0 \\ 0 \\ 0 \\ 0 \\ 0 \end{Bmatrix} \tag{5.39}$$

and

$$\{\boldsymbol{\varepsilon}^{\boldsymbol{e}}\} = \begin{Bmatrix} \varepsilon_{xx}{}^{e} \\ \varepsilon_{yy}{}^{e} \\ \gamma_{xy}{}^{e} \\ \varepsilon_{zz}{}^{e} \\ \gamma_{yz}{}^{e} \\ \gamma_{zx}{}^{e} \end{Bmatrix}. \tag{5.40}$$

Therefore, substituting Equations 5.14, 5.39, and 5.40 into Equation 5.2 yields

$$\begin{Bmatrix} \sigma_{xx} \\ 0 \\ 0 \\ 0 \\ 0 \\ 0 \end{Bmatrix} = \frac{E}{(1+\nu)(1-2\nu)} \begin{bmatrix} (1-\nu) & \nu & 0 & \nu & 0 & 0 \\ \nu & (1-\nu) & 0 & \nu & 0 & 0 \\ 0 & 0 & \frac{(1-2\nu)}{2} & 0 & 0 & 0 \\ \nu & \nu & 0 & (1-\nu) & 0 & 0 \\ 0 & 0 & 0 & 0 & \frac{(1-2\nu)}{2} & 0 \\ 0 & 0 & 0 & 0 & 0 & \frac{(1-2\nu)}{2} \end{bmatrix} \begin{Bmatrix} \varepsilon_{xx}{}^{e} \\ \varepsilon_{yy}{}^{e} \\ \gamma_{xy}{}^{e} \\ \varepsilon_{zz}{}^{e} \\ \gamma_{yz}{}^{e} \\ \gamma_{zx}{}^{e} \end{Bmatrix}. \tag{5.41}$$

Using linear algebra, we can partition Equation 5.41 as follows:

$$\left[\begin{array}{c|c} \sigma_{xx} & \\ 0 & \\ 0 & \\ 0 & \\ 0 & \\ 0 & \end{array}\right] = \left[\begin{array}{c|ccccc} (1-\nu) & \nu & 0 & \nu & 0 & 0 \\ \nu & (1-\nu) & 0 & \nu & 0 & 0 \\ 0 & 0 & \frac{(1-2\nu)}{2} & 0 & 0 & 0 \\ \nu & \nu & 0 & (1-\nu) & 0 & 0 \\ 0 & 0 & 0 & 0 & \frac{(1-2\nu)}{2} & 0 \\ 0 & 0 & 0 & 0 & 0 & \frac{(1-2\nu)}{2} \end{array}\right] \left\{\begin{array}{c} \varepsilon_{xx}{}^{e} \\ \varepsilon_{yy}{}^{e} \\ \gamma_{xy}{}^{e} \\ \varepsilon_{zz}{}^{e} \\ \gamma_{yz}{}^{e} \\ \gamma_{zx}{}^{e} \end{array}\right\}$$

$$\left[\begin{array}{c|c} \sigma_{xx} & \\ 0 & \\ 0 & \\ 0 & \\ 0 & \\ 0 & \end{array}\right] = \left[\begin{array}{c|c} [D_{AA}] & [D_{AB}] \\ [D_{BA}] & [D_{BB}] \end{array}\right] \left\{\begin{array}{c} \varepsilon_{xx}{}^{e} \\ \varepsilon_{yy}{}^{e} \\ \gamma_{xy}{}^{e} \\ \varepsilon_{zz}{}^{e} \\ \gamma_{yz}{}^{e} \\ \gamma_{zx}{}^{e} \end{array}\right\}$$

where

$$[D_{AA}] = \frac{E}{(1+\nu)(1-2\nu)}[(1-\nu)] \tag{5.42}$$

$$[D_{AB}] = \frac{E}{(1+\nu)(1-2\nu)}[\nu \quad 0 \quad \nu \quad 0 \quad 0] \tag{5.43}$$

$$[D_{BA}] = \frac{E}{(1+\nu)(1-2\nu)}\begin{bmatrix}\nu\\0\\\nu\\0\\0\end{bmatrix} \tag{5.44}$$

$$[D_{BB}] = \frac{E}{(1+\nu)(1-2\nu)}\begin{bmatrix}(1-\nu) & 0 & \nu & 0 & 0\\ 0 & \frac{(1-2\nu)}{2} & 0 & 0 & 0\\ \nu & 0 & (1-\nu) & 0 & 0\\ 0 & 0 & 0 & \frac{(1-2\nu)}{2} & 0\\ 0 & 0 & 0 & 0 & \frac{(1-2\nu)}{2}\end{bmatrix} \tag{5.45}$$

We can now represent Equation 5.41 with two linearly independent equations:

$$\{\sigma_{xx}\} = [D_{AA}]\{{\varepsilon_{xx}}^{e}\} + [D_{AB}]\begin{Bmatrix}{\varepsilon_{yy}}^{e}\\{\gamma_{xy}}^{e}\\{\varepsilon_{zz}}^{e}\\{\gamma_{yz}}^{e}\\{\gamma_{zx}}^{e}\end{Bmatrix} \tag{5.46}$$

and

$$\begin{Bmatrix}0\\0\\0\\0\\0\end{Bmatrix} = [D_{BA}]\{{\varepsilon_{xx}}^{e}\} + [D_{BB}]\begin{Bmatrix}{\varepsilon_{yy}}^{e}\\{\gamma_{xy}}^{e}\\{\varepsilon_{zz}}^{e}\\{\gamma_{yz}}^{e}\\{\gamma_{zx}}^{e}\end{Bmatrix}. \tag{5.47}$$

Rearranging Equation 5.47 solves for the out-of-axis elastic strains in terms of the elastic in-axis strain,

$$\begin{Bmatrix} {\varepsilon_{yy}}^{e} \\ {\gamma_{xy}}^{e} \\ {\varepsilon_{zz}}^{e} \\ {\gamma_{yz}}^{e} \\ {\gamma_{zx}}^{e} \end{Bmatrix} = -[D_{BB}]^{-1}[D_{BA}]\{{\varepsilon_{xx}}^{e}\}. \tag{5.48}$$

Therefore, the total elastic strain can be expressed as a function of $\{{\varepsilon_{xx}}^{e}\}$,

$$\{\boldsymbol{\varepsilon^{e}}\} = \begin{Bmatrix} {\varepsilon_{xx}}^{e} \\ {\varepsilon_{yy}}^{e} \\ {\gamma_{xy}}^{e} \\ {\varepsilon_{zz}}^{e} \\ {\gamma_{yz}}^{e} \\ {\gamma_{zx}}^{e} \end{Bmatrix} = \begin{Bmatrix} \begin{bmatrix} 1 \\ -[D_{BB}]^{-1}[D_{BA}] \end{bmatrix} \end{Bmatrix} \{{\varepsilon_{xx}}^{e}\}. \tag{5.49}$$

Now if we pre-multiply both sides of Equation 5.49 by the full $[N]$ matrix (Equation 4.21), we solve for the particle elastic stretch state all eighteen pd-bonds in terms of the elastic axial strain,

$$\{\boldsymbol{S^{e}}\} = [N]\begin{Bmatrix} \begin{bmatrix} 1 \\ -[D_{BB}]^{-1}[D_{BA}] \end{bmatrix} \end{Bmatrix} \{{\varepsilon_{xx}}^{e}\}. \tag{5.50}$$

By substituting in Equation 5.18 for the elastic axial, we now have a relationship that expresses the total stretch state of the particle in terms of the two elastic axial pd-bond stretches,

$$\{\boldsymbol{S^{e}}\} = [N]\begin{Bmatrix} \begin{bmatrix} 1 \\ -[D_{BB}]^{-1}[D_{BA}] \end{bmatrix} \end{Bmatrix} [N']\{\boldsymbol{S'^{e}}\}. \tag{5.51}$$

We define the matrix $[C]$ which converts the simplified elastic stretch state to the full elastic stretch state,

$$[C] = [N]\left\{\begin{bmatrix} 1 \\ -[D_{BB}]^{-1}[D_{BA}] \end{bmatrix}\right\}[N'] \tag{5.52}$$

Substituting Equations 4.21, 5.28, 5.44, and 5.45 into Equation 5.52 yields, using MatLab,

$$[C] = \frac{1}{8}\begin{bmatrix} 4 & 4 \\ 4 & 4 \\ (1-3v) & (1-3v) \\ (1-3v) & (1-3v) \\ (1-3v) & (1-3v) \\ (1-3v) & (1-3v) \\ (1-3v) & (1-3v) \\ (1-3v) & (1-3v) \\ (1-3v) & (1-3v) \\ -4v & -4v \\ -4v & -4v \\ (2-2v) & (2-2v) \\ (2-2v) & (2-2v) \\ -4v & -4v \\ -4v & -4v \\ (2-2v) & (2-2v) \\ (2-2v) & (2-2v) \end{bmatrix}. \tag{5.53}$$

Therefore, we now express the full elastic stretch state of the particle as a function the simplified uniaxial one-dimensional elastic stretch state.

5.6 SPLM stretch state for 2D hexagonal lattice layer, plane stress

Consider a solid body with a constant thickness t_{BODY}, is un-constrained in the out-of-plane direction, and is subjected to body forces in the in-plane directions. Under these

conditions, the SPLM three-dimensional model can be simplified to a two-dimensional lattice plane of particles. The thickness of this lattice layer is the tributary thickness of a SPLM particle, $t_{LAYER} = \sqrt{\frac{2}{3}}L$. Therefore the in-plane forces imposed on this layer of particles, $\{F_{LAYER}\}$, is proportional to the in-plane forces imposed on the body, $\{F_{BODY}\}$, with respect to the body's cross-sectional thickness,

$$\{F_{LAYER}\} = \{F_{BODY}\}\left(\frac{t_{LAYER}}{t_{BODY}}\right). \tag{5.54}$$

Similar to a SPLM strand particle, a SPLM particle in a lattice layer still had eighteen pd-bonds in- and out-of-plane with the layer. The stretches of pd-bonds in the out of plane direction are non-zero and, while the net forces on the particle in the out of plane direction are zero, the pd-bonds in the out of plane direction do have forces in them. Therefore, we must solve for the elastic stretch state of all eighteen pd-bonds in terms of the six in-plane elastic pd-bonds stretches.

In classical mechanics, the stress and elastic strain for two-dimensional plane stress are expressed as

$$\{\boldsymbol{\sigma}\} = \begin{Bmatrix} \sigma_{xx} \\ \sigma_{yy} \\ \tau_{xy} \\ 0 \\ 0 \\ 0 \end{Bmatrix} \tag{5.55}$$

and

$$\{\boldsymbol{\varepsilon}^{\boldsymbol{e}}\} = \begin{Bmatrix} \varepsilon_{xx}{}^{e} \\ \varepsilon_{yy}{}^{e} \\ \gamma_{xy}{}^{e} \\ \varepsilon_{zz}{}^{e} \\ \gamma_{yz}{}^{e} \\ \gamma_{zx}{}^{e} \end{Bmatrix}. \tag{5.56}$$

Then, using linear algebra, we partition the classical constitutive relationship as follows:

$$\left\{\begin{matrix} \sigma_{xx} \\ \sigma_{yy} \\ \tau_{xy} \\ 0 \\ 0 \\ 0 \end{matrix}\right\} = \frac{E}{(1+\nu)(1-2\nu)} \left[\begin{array}{ccc:ccc} (1-\nu) & \nu & 0 & \nu & 0 & 0 \\ \nu & (1-\nu) & 0 & \nu & 0 & 0 \\ 0 & 0 & \frac{(1-2\nu)}{2} & 0 & 0 & 0 \\ \hdashline \nu & \nu & 0 & (1-\nu) & 0 & 0 \\ 0 & 0 & 0 & 0 & \frac{(1-2\nu)}{2} & 0 \\ 0 & 0 & 0 & 0 & 0 & \frac{(1-2\nu)}{2} \end{array}\right] \left\{\begin{matrix} \varepsilon_{xx}{}^{e} \\ \varepsilon_{yy}{}^{e} \\ \gamma_{xy}{}^{e} \\ \varepsilon_{zz}{}^{e} \\ \gamma_{yz}{}^{e} \\ \gamma_{zx}{}^{e} \end{matrix}\right\} \tag{5.57}$$

$$\left\{\begin{matrix} \sigma_{xx} \\ \sigma_{yy} \\ \tau_{xy} \\ 0 \\ 0 \\ 0 \end{matrix}\right\} = \left[\begin{array}{c:c} [D_{AA}] & [D_{AB}] \\ \hdashline [D_{BA}] & [D_{BB}] \end{array}\right] \left\{\begin{matrix} \varepsilon_{xx}{}^{e} \\ \varepsilon_{yy}{}^{e} \\ \gamma_{xy}{}^{e} \\ \varepsilon_{zz}{}^{e} \\ \gamma_{yz}{}^{e} \\ \gamma_{zx}{}^{e} \end{matrix}\right\}$$

where

$$[D_{AA}] = \frac{E}{(1+\nu)(1-2\nu)} \begin{bmatrix} (1-\nu) & \nu & 0 \\ \nu & (1-\nu) & 0 \\ 0 & 0 & \frac{(1-2\nu)}{2} \end{bmatrix} \tag{5.58}$$

$$[D_{AB}] = \frac{E}{(1+\nu)(1-2\nu)} \begin{bmatrix} \nu & 0 & 0 \\ \nu & 0 & 0 \\ 0 & 0 & 0 \end{bmatrix} \tag{5.59}$$

$$[D_{BA}] = \frac{E}{(1+\nu)(1-2\nu)}\begin{bmatrix} \nu & \nu & 0 \\ 0 & 0 & 0 \\ 0 & 0 & 0 \end{bmatrix} \tag{5.60}$$

$$[D_{BB}] = \frac{E}{(1+\nu)(1-2\nu)}\begin{bmatrix} (1-\nu) & 0 & 0 \\ 0 & \frac{(1-2\nu)}{2} & 0 \\ 0 & 0 & \frac{(1-2\nu)}{2} \end{bmatrix} \tag{5.61}$$

We can now represent Equation 5.57 with two linearly independent equations:

$$\begin{Bmatrix} \sigma_{xx} \\ \sigma_{yy} \\ \tau_{xy} \end{Bmatrix} = [D_{AA}]\begin{Bmatrix} {\varepsilon_{xx}}^e \\ {\varepsilon_{yy}}^e \\ {\gamma_{xy}}^e \end{Bmatrix} + [D_{AB}]\begin{Bmatrix} {\varepsilon_{zz}}^e \\ {\gamma_{yz}}^e \\ {\gamma_{zx}}^e \end{Bmatrix} \tag{5.62}$$

and

$$\begin{Bmatrix} 0 \\ 0 \\ 0 \end{Bmatrix} = [D_{BA}]\begin{Bmatrix} {\varepsilon_{xx}}^e \\ {\varepsilon_{yy}}^e \\ {\gamma_{xy}}^e \end{Bmatrix} + [D_{BB}]\begin{Bmatrix} {\varepsilon_{zz}}^e \\ {\gamma_{yz}}^e \\ {\gamma_{zx}}^e \end{Bmatrix}. \tag{5.63}$$

We now solve for the out-of-plane elastic strains in terms of the in-plane elastic strains from Equation 5.63,

$$\begin{Bmatrix} {\varepsilon_{zz}}^e \\ {\gamma_{yz}}^e \\ {\gamma_{zx}}^e \end{Bmatrix} = -[D_{BB}]^{-1}[D_{BA}]\begin{Bmatrix} {\varepsilon_{xx}}^e \\ {\varepsilon_{yy}}^e \\ {\gamma_{xy}}^e \end{Bmatrix}. \tag{5.64}$$

The total elastic strains can be expressed in terms of the in-plane elastic strains by

$$\{\boldsymbol{\varepsilon^e}\} = \begin{Bmatrix} {\varepsilon_{xx}}^e \\ {\varepsilon_{yy}}^e \\ {\gamma_{xy}}^e \\ {\varepsilon_{zz}}^e \\ {\gamma_{yz}}^e \\ {\gamma_{zx}}^e \end{Bmatrix} = \begin{Bmatrix} 1 & 0 & 0 \\ 0 & 1 & 0 \\ 0 & 0 & 1 \\ \multicolumn{3}{c}{\left[-[D_{BB}]^{-1}[D_{BA}]\right]} \end{Bmatrix}\begin{Bmatrix} {\varepsilon_{zz}}^e \\ {\gamma_{yz}}^e \\ {\gamma_{zx}}^e \end{Bmatrix}. \tag{5.65}$$

Pre-multiplying both sides of Equation 5.65 by the fully $[N]$ matrix, Equation 4.21, yields

$$\{\boldsymbol{S^e}\} = [N]\begin{Bmatrix} {\varepsilon_{xx}}^e \\ {\varepsilon_{yy}}^e \\ {\gamma_{xy}}^e \\ {\varepsilon_{zz}}^e \\ {\gamma_{yz}}^e \\ {\gamma_{zx}}^e \end{Bmatrix} = [N]\begin{Bmatrix} 1 & 0 & 0 \\ 0 & 1 & 0 \\ 0 & 0 & 1 \\ \begin{bmatrix} -[D_{BB}]^{-1}[D_{BA}] \end{bmatrix} \end{Bmatrix}\begin{Bmatrix} {\varepsilon_{zz}}^e \\ {\gamma_{yz}}^e \\ {\gamma_{zx}}^e \end{Bmatrix}. \tag{5.66}$$

Using Equation 5.##, we can represent the elastic in-plane strain with the elastic in-plane stretches,

$$\{\boldsymbol{S^e}\} = [N]\begin{Bmatrix} 1 & 0 & 0 \\ 0 & 1 & 0 \\ 0 & 0 & 1 \\ \begin{bmatrix} -[D_{BB}]^{-1}[D_{BA}] \end{bmatrix} \end{Bmatrix}[N']\{\boldsymbol{S'^e}\}, \tag{5.67}$$

Therefore, $[C]$ for two-dimensional plane stress is

$$[C] = [N]\begin{Bmatrix} 1 & 0 & 0 \\ 0 & 1 & 0 \\ 0 & 0 & 1 \\ \begin{bmatrix} -[D_{BB}]^{-1}[D_{BA}] \end{bmatrix} \end{Bmatrix}[N']\,. \tag{5.68}$$

Substituting Equations 4.21, 5.36, 5.60, and 5.61 into Equation 5.68 yields, using MatLab,

$$[C] = \frac{1}{24}\begin{bmatrix} 12 & 12 & 0 & 0 & 0 & 0 \\ 12 & 12 & 0 & 0 & 0 & 0 \\ 3 & 3 & 9 & 9 & 3\sqrt{3} & 3\sqrt{3} \\ 3 & 3 & 9 & 9 & 3\sqrt{3} & 3\sqrt{3} \\ 3 & 3 & 9 & 9 & -3\sqrt{3} & -3\sqrt{3} \\ 3 & 3 & 9 & 9 & -3\sqrt{3} & -3\sqrt{3} \\ \left(\frac{8}{v-1}+11\right) & \left(\frac{8}{v-1}+11\right) & \left(\frac{8}{v-1}+9\right) & \left(\frac{8}{v-1}+9\right) & \sqrt{3} & \sqrt{3} \\ \left(\frac{8}{v-1}+11\right) & \left(\frac{8}{v-1}+11\right) & \left(\frac{8}{v-1}+9\right) & \left(\frac{8}{v-1}+9\right) & \sqrt{3} & \sqrt{3} \\ \left(\frac{8}{v-1}+11\right) & \left(\frac{8}{v-1}+11\right) & \left(\frac{8}{v-1}+9\right) & \left(\frac{8}{v-1}+9\right) & -\sqrt{3} & -\sqrt{3} \\ \left(\frac{8}{v-1}+11\right) & \left(\frac{8}{v-1}+11\right) & \left(\frac{8}{v-1}+9\right) & \left(\frac{8}{v-1}+9\right) & -\sqrt{3} & -\sqrt{3} \\ \left(\frac{8}{v-1}+8\right) & \left(\frac{8}{v-1}+8\right) & \left(\frac{8}{v-1}+12\right) & \left(\frac{8}{v-1}+12\right) & 0 & 0 \\ \left(\frac{8}{v-1}+8\right) & \left(\frac{8}{v-1}+8\right) & \left(\frac{8}{v-1}+12\right) & \left(\frac{8}{v-1}+12\right) & 0 & 0 \\ \left(\frac{4}{v-1}+10\right) & \left(\frac{4}{v-1}+10\right) & \left(\frac{4}{v-1}+6\right) & \left(\frac{4}{v-1}+6\right) & 2\sqrt{3} & 2\sqrt{3} \\ \left(\frac{4}{v-1}+10\right) & \left(\frac{4}{v-1}+10\right) & \left(\frac{4}{v-1}+6\right) & \left(\frac{4}{v-1}+6\right) & 2\sqrt{3} & 2\sqrt{3} \\ \left(\frac{4}{v-1}+4\right) & \left(\frac{4}{v-1}+4\right) & \left(\frac{4}{v-1}+12\right) & \left(\frac{4}{v-1}+12\right) & 0 & 0 \\ \left(\frac{4}{v-1}+4\right) & \left(\frac{4}{v-1}+4\right) & \left(\frac{4}{v-1}+12\right) & \left(\frac{4}{v-1}+12\right) & 0 & 0 \\ \left(\frac{4}{v-1}+10\right) & \left(\frac{4}{v-1}+10\right) & \left(\frac{4}{v-1}+6\right) & \left(\frac{4}{v-1}+6\right) & -2\sqrt{3} & -2\sqrt{3} \\ \left(\frac{4}{v-1}+10\right) & \left(\frac{4}{v-1}+10\right) & \left(\frac{4}{v-1}+6\right) & \left(\frac{4}{v-1}+6\right) & -2\sqrt{3} & -2\sqrt{3} \end{bmatrix}. \quad (5.69)$$

Therefore, we can now determine the full elastic stretch state from the six in plane elastic stretches under plane stress conditions.

5.7 SPLM stretch state for 2D hexagonal lattice layer, plane strain

The SPLM special plane strain case is last special case we will consider. Under plane strain conditions, we assume that the total out-of-plane strain, ${\varepsilon_{zz}}^T$, is zero. However, this does not necessarily mean that the out-of-plane elastic strain, ${\varepsilon_{zz}}^e$, is zero. The total out-of-plane strain is a function of the out-of-plane elastic strain plus the out-of-plane plastic strain, ${\varepsilon_{zz}}^p$,

$${\varepsilon_{zz}}^T = {\varepsilon_{zz}}^e + {\varepsilon_{zz}}^p = 0. \quad (5.70)$$

Therefore, if the total out-of-plane strain is zero per plane strain conditions, the out-of-plane elastic strain is a function of the out-of-plane plastic strain,

$$\varepsilon_{zz}{}^{e} = -\varepsilon_{zz}{}^{p}. \tag{5.71}$$

If we know the out-of-plane elastic strains, we can find the in-plane elastic strains from Equation 5.35,

$$\{\boldsymbol{\varepsilon^e}\} = \begin{Bmatrix} \begin{Bmatrix} \varepsilon_{xx}{}^{e} \\ \varepsilon_{yy}{}^{e} \\ \gamma_{xy}{}^{e} \end{Bmatrix} = \begin{bmatrix} 1/2 & 1/2 & 0 & 0 & 0 & 0 \\ -1/6 & -1/6 & 1/3 & 1/3 & 1/3 & 1/3 \\ 0 & 0 & 1/\sqrt{3} & 1/\sqrt{3} & -1/\sqrt{3} & -1/\sqrt{3} \end{bmatrix} \begin{Bmatrix} S_1{}^{e} \\ S_2{}^{e} \\ S_3{}^{e} \\ S_4{}^{e} \\ S_5{}^{e} \\ S_6{}^{e} \end{Bmatrix} \\ \begin{Bmatrix} \varepsilon_{zz}{}^{e} = -\varepsilon_{zz}{}^{p} \\ \gamma_{yz}{}^{e} = 0 \\ \gamma_{zx}{}^{e} = 0 \end{Bmatrix} \end{Bmatrix}. \tag{5.72}$$

With the elastic strains known, we can solve for the all eighteen elastic stretches by pre-multiplying Equation 5.72 by the full $[N]$ matrix.

5.8 SPLM force state for 1D uniaxial lattice strand

In the case of one dimensional uniaxial force, we assume that the in-axis pd-bond force, F_i, is equal to the in-axis elastic pd-bond stretch, $S_i{}^{e}$, multiplied the constant a,

$$F_i = aS_i{}^{e}. \tag{5.73}$$

In matrix form, Equation 5.73 is expressed as

$$\begin{Bmatrix} F_1 \\ F_2 \end{Bmatrix} = \begin{bmatrix} a & 0 \\ 0 & a \end{bmatrix} \begin{Bmatrix} S_1{}^{e} \\ S_2{}^{e} \end{Bmatrix}, \tag{5.74}$$

thus

$$[K] = \begin{bmatrix} a & 0 \\ 0 & a \end{bmatrix}. \tag{5.75}$$

The one-dimensional classical mechanics constitutive matrix $[D]$ for an isotropic bar with cross sectional area A in a homogeneous state of uniaxial stress is simply equal to the modulus of elasticity E of the material,

$$[D] = E. \tag{5.76}$$

Recall from section 5.4, for the one dimensional case, $[N]$ is

$$[N] = \begin{bmatrix} 1 \\ 1 \end{bmatrix}, \tag{5.24}$$

therefore, using Equation 4.7, $[M]$ is

$$[M] = \frac{\sqrt{2}}{L^2} \begin{bmatrix} 1 & 1 \end{bmatrix}. \tag{5.77}$$

Substituting Equations 5.24, 5.75, 5.76, and 5.77 into Equation 5.9 and reducing yields

$$E = \frac{1}{\sqrt{2}L^2} \begin{bmatrix} 1 & 1 \end{bmatrix} \begin{bmatrix} a & 0 \\ 0 & a \end{bmatrix} \begin{bmatrix} 1 \\ 1 \end{bmatrix} = \frac{1}{\sqrt{2}L^2} \begin{bmatrix} a & a \end{bmatrix} \begin{bmatrix} 1 \\ 1 \end{bmatrix} = \frac{\sqrt{2}}{L^2} a. \tag{5.78}$$

Solving Equation 5.78 for a yields

$$a = \frac{L^2}{\sqrt{2}} \cdot E. \tag{5.79}$$

When $a = \frac{L^2}{\sqrt{2}} \cdot E$ for our assumed solution (Equation 5.74), there is energy equivalence between $[K]$ and $[D]$ for one dimensional uniaxial force. As stated previously, the out-of-axis pd-bonds do have force in them; however their net force in the out of axis direction is zero. Therefore only the two in-axis pd-bonds are considered for the one-dimensional uniaxial case.

5.9 SPLM force state for 2D hexagonal lattice layer, plane stress

Under plane stress conditions for a tributary layer of particles, we now assume that the pd-bond force, F_i, is a function of the elastic pd-bond stretch, ${S_i}^e$, multiplied by the constant a plus the average elastic pd-bond stetches, ${S_{AVG}}^e$, of the six in-plane nearest neighboring pd-bonds multiplied by the constant b,

$$F_i = a{S_i}^e + b{S_{AVG}}^e, \tag{5.80}$$

where

$${S_{AVG}}^e = \frac{1}{6}\sum_{i=1}^{6} {S_i}^e. \tag{5.81}$$

Expanding Equation 5.80 into matrix form,

$$\begin{Bmatrix} F_1 \\ F_2 \\ F_3 \\ F_4 \\ F_5 \\ F_6 \end{Bmatrix} = \begin{bmatrix} a+b/6 & b/6 & b/6 & b/6 & b/6 & b/6 \\ b/6 & a+b/6 & b/6 & b/6 & b/6 & b/6 \\ b/6 & b/6 & a+b/6 & b/6 & b/6 & b/6 \\ b/6 & b/6 & b/6 & a+b/6 & b/6 & b/6 \\ b/6 & b/6 & b/6 & b/6 & a+b/6 & b/6 \\ b/6 & b/6 & b/6 & b/6 & b/6 & a+b/6 \end{bmatrix} \begin{Bmatrix} {S_1}^e \\ {S_2}^e \\ {S_3}^e \\ {S_4}^e \\ {S_5}^e \\ {S_6}^e \end{Bmatrix}, \tag{5.82}$$

therefore,

$$[K] = \begin{bmatrix} a+b/6 & b/6 & b/6 & b/6 & b/6 & b/6 \\ b/6 & a+b/6 & b/6 & b/6 & b/6 & b/6 \\ b/6 & b/6 & a+b/6 & b/6 & b/6 & b/6 \\ b/6 & b/6 & b/6 & a+b/6 & b/6 & b/6 \\ b/6 & b/6 & b/6 & b/6 & a+b/6 & b/6 \\ b/6 & b/6 & b/6 & b/6 & b/6 & a+b/6 \end{bmatrix}. \tag{5.83}$$

From classical mechanics we know that the constitutive relationship $[D]$ between in-plane stress and in-plane strain, assuming plane stress conditions, is

$$[D] = \frac{E}{1-v^2}\begin{bmatrix} 1 & v & 0 \\ v & 1 & 0 \\ 0 & 0 & \frac{(1-v)}{2} \end{bmatrix}, \tag{5.84}$$

Recall from section 5.4, for the two-dimensional case, $[N]$ is

$$[N] = \begin{bmatrix} 1 & 0 & 0 \\ 1 & 0 & 0 \\ 1/4 & 3/4 & \sqrt{3}/4 \\ 1/4 & 3/4 & \sqrt{3}/4 \\ 1/4 & 3/4 & -\sqrt{3}/4 \\ 1/4 & 3/4 & -\sqrt{3}/4 \end{bmatrix}. \tag{5.31}$$

therefore, using Equation 4.7, $[M]$ is

$$[M] = \frac{1}{\sqrt{2}L^2}\begin{bmatrix} 1 & 1 & 1/4 & 1/4 & 1/4 & 1/4 \\ 0 & 0 & 3/4 & 3/4 & 3/4 & 3/4 \\ 0 & 0 & \sqrt{3}/4 & \sqrt{3}/4 & -\sqrt{3}/4 & -\sqrt{3}/4 \end{bmatrix}. \tag{5.85}$$

Thus, we substitute Equations 5.31, 5.83, 5.84, and 5.85 into Equation 5.9 and reduce. Using Matlab to solve, we obtain

$$\frac{E}{1-v^2}\begin{bmatrix} 1 & v & 0 \\ v & 1 & 0 \\ 0 & 0 & \frac{(1-v)}{2} \end{bmatrix} = \frac{3\sqrt{2}}{8L^2}\begin{bmatrix} 3a+2b & a+2b & 0 \\ a+2b & 3a+2b & 0 \\ 0 & 0 & a \end{bmatrix}. \tag{5.86}$$

Same as in the three dimensional case, we set corresponding elements equal to each other from Equation 5.86; this produces two linear equations with two unknowns, a and b. Solving,

$$a = \frac{2\sqrt{2}}{3} \cdot \frac{EL^2}{(v+1)}, \tag{5.87}$$

$$b = \frac{\sqrt{2}}{3} \cdot \frac{EL^2(1-3v)}{(v^2-1)}. \tag{5.88}$$

Substituting in Equations 5.87 and 5.88 into Equation 5.83 yields a SPLM linear elastic constitutive matrix $[K]$ that corresponds with the plane stress classical linear elastic constitutive matrix $[D]$. While the out-of-plane pd-bonds do carry forces, the net force in the out-of-plane direction is zero. Thus, we only consider the six in-plane nearest neighboring bonds for the two-dimensional plane stress case.

5.10 Summary

In this chapter, we have developed valid SPLM linear elastic relationships for one-dimensional uniaxial, two-dimensional plane stress and plane strain, and three dimensional cases. We require that when there exists a homogenous strain field and small deformations that these relationships correspond to linear elastic classical mechanics. The constitutive relationships defined in the previous sections for each case fulfill this requirement. Note that other solutions exist. For example, it can be shown that another possible solution for the two dimensional plane stress case is that the pd-bond force state is equal to the elastic pd-bond stretch state multiplied by a constant plus the sum of the elastic stretches in the adjacent pd-bonds multiplied by different constant,

$$F_i = aS_i{}^e + b\sum S_{adjacent}{}^e. \tag{5.89}$$

For all cases, we have chosen solutions that we believe are the most computationally efficient, but other valid constitutive relationships could be chosen.

It is possible that our assumed elastic solution for the full three-dimensional case is flawed. From examples performed using the three dimensinal SPLM linear elastic theory developed in this chapter, we know that our results do not match the classical solution. Because we have derived SPLM linear elastic theory from the classic linear elastic theory, SPLM should

match the classical mechanics solution when a comparison between the two models can be made. Therefore more research is necessary to correct the three dimensional SPLM linear elastic theory. But on a more encouraging note, the one-dimensional uniaxial and two-dimensional plane stress SPLM models are yielding good results when compared with the classical solutions.

The relationships developed in this chapter are only valid for infinitesimal linear elastic deformations. However, a fundamental goal of SPLM is to also model large deformations, plasticity, and damage beyond the elastic limit. In Chapter 6 we present a SPLM plasticity model.

Chapter 6

SPLM Plasticity

6.1 Introduction

In this chapter we develop an isochoric plasticity model for the state-based peridynamic lattice model (SPLM) equivalent to a J2 plasticity model. We assume, for plastically deformable material, that a SPLM particle behaves elastic-perfectly plastically. SPLM plasticity could be modeled using different assumptions, i.e. work hardening; however for this thesis we only derive the elastic-perfectly plastic relationship between pd-bond force state and pd-bond stretch state. There are two fundamental relationships we need to establish to define our SPLM plasticity theory: a SPLM particle yield criterion and pd-bond stretch state flow rule in the plastic region.

In classical mechanics, it is assumed that the yield criterion is a function of the deviatoric stress; the hydrostatic stress does not affect yielding. We assume this also for SPLM. We assume that a SPLM particle will yield as a function of the deviatoric particle force state and independent of the hydrostatic particle force state.

In 1930 the Prandtl-Reuss stress-strain relationships for elastic-perfectly plastic materials were introduced [10]. They proposed that the plastic strain rate of flow is proportional to the deviatoric stress. From the relationships developed in Chapter 4 and under conditions were a comparison between SPLM and classical mechanics can be made, we can expand a SPLM pd-bond force state – pd-bond stretch state relationships from the Prandtl-Reuss stress-strain relationships. From experimental observations we know that there is no volumetric strain due to plastic deformation. The Prandtl-Reuss relationships assume plastic incompressibility. SPLM

plasticity has been expanded from the Prandtl-Reuss plasticity model; thus, SPLM plasticity will also not allow volumetric changes due to plastic deformation.

6.2 SPLM yield criteria

SPLM assumes that a pd-bond will yield when the force state equals or exceeds the material pd-bond yield force, f_y. In classical mechanics, the yield stress, σ_y, has been defined for virtually all material types. Therefore, when a comparison between SPLM and classical mechanics can be made, we can determine a corresponding pd-bond yield force from the yield stress. Consider a three dimensional SPLM particle under a uniaxial state of stress, shown in Figure 6.1 (the second-nearest pd-bonds are not shown for figure clarity). The particle is free to contract in the out-of-axis direction and while the force in individual out-of-axis pd-bonds is not zero, the net sum of the all components of the out of axis forces are zero,

$$\sum F_{3,x} + F_{3,y} + F_{3,z} + \cdots + F_{18,x} + F_{18,y} + F_{18,z} = 0. \tag{6.1}$$

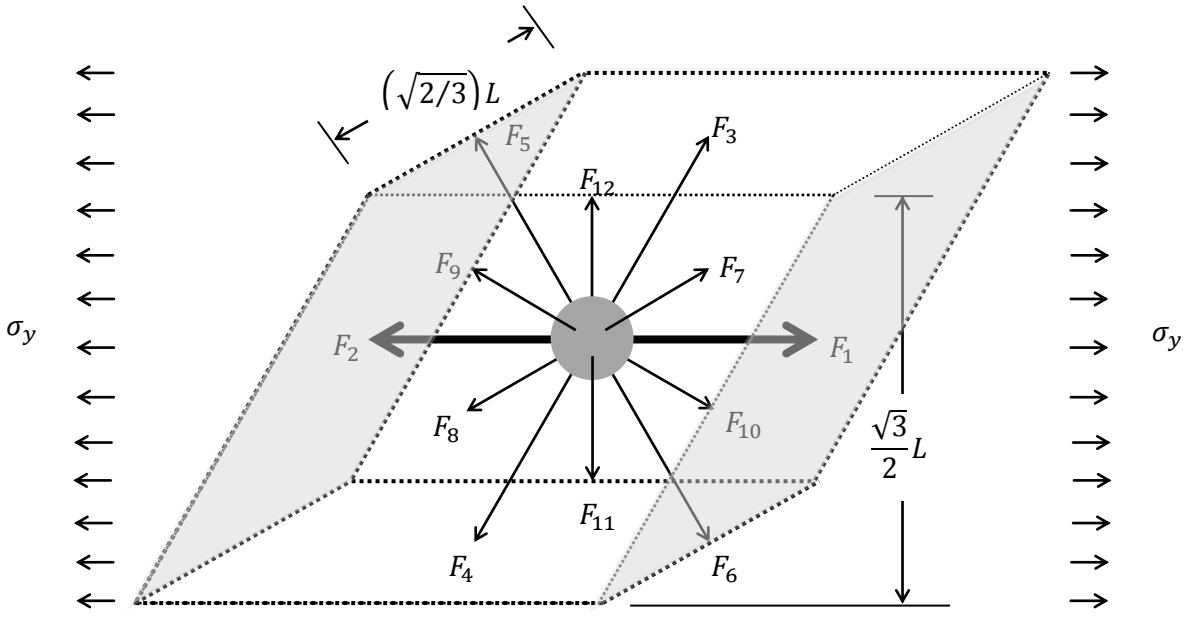

Figure 6.1 3D SPLM particle under uniaxial stress

The particle is yielding therefore the two remaining pd-bond force states, which are normal to the plane at which the yield stress is being applied and have no force component in the out of axis directions, must be equal to the yield link force state,

$$F_{1,x} = F_{2,x} = f_y. \tag{6.2}$$

The corresponding pd-bond yield force would be equal to the yield stress multiplied by the tributary area normal to the stress,

$$f_y = \sigma_y \cdot A_{Normal} = \sigma_y \left(\frac{\sqrt{3}}{2}L\right)\left(\sqrt{\frac{2}{3}}L\right),$$

$$f_y = \sigma_y \cdot \frac{L^2}{\sqrt{2}}. \tag{6.3}$$

With the pd-bond yield force state determined, we now develop the SPLM particle yield criteria. If we were to make a cut in the particle, dividing it into two equal halves, we would have three orthogonal components of force necessary for equilibrium. We call these three components the particle force state, $\{F_p\}$,

$$\{F_p\} = \begin{Bmatrix} F_x \\ F_y \\ F_z \end{Bmatrix}. \tag{6.4}$$

As previously stated, we assume that a SPLM particle will yield as a function of the deviatoric particle force state, $\{F_{Dev}\}$. We define $\{F_{Dev}\}$ to be equal to the particle force state, $\{F_p\}$, minus the average particle force state, F_{Avg},

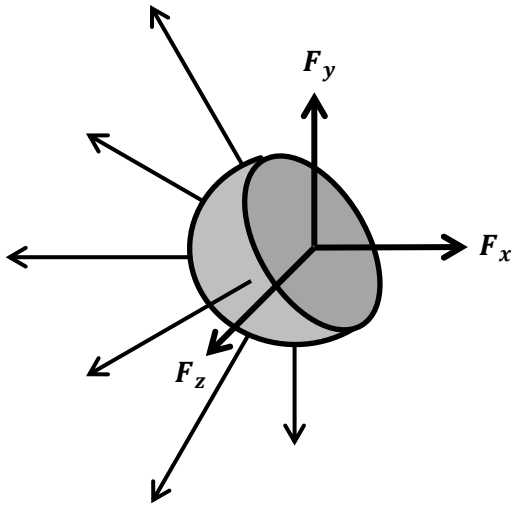

Figure 6.2 FBD particle force state

$$\{F_{Dev}\} = \begin{Bmatrix} F_x - F_{Avg} \\ F_y - F_{Avg} \\ F_z - F_{Avg} \end{Bmatrix}, \tag{6.5}$$

where F_{Avg} is

$$F_{Avg} = \frac{F_x + F_y + F_z}{3}. \tag{6.6}$$

We define the normalized deviatoric particle force state, $F_{NormDev}$, is equal to the square root of the sum of the squares of deviatoric particle force state,

$$F_{NormDev} = \sqrt{\left(F_x - F_{Avg}\right)^2 + \left(F_y - F_{Avg}\right)^2 + \left(F_z - F_{Avg}\right)^2}\ . \tag{6.7}$$

We assume that when $F_{NormDev}$ equals or exceeds the yield normalized deviatoric particle force state, $(F_{NormDev})_y$, the particle will yield,

$$F_{NormDev} \geq (F_{NormDev})_y. \tag{6.8}$$

We now can determine the yield normalized deviatoric particle force state as a function of the pd-bond yield force state,

$$(F_{NormDev})_y = f(f_y). \tag{6.9}$$

Let us again consider the SPLM particle in a state of uniaxial force. We assume that the particle is yielding, thus we can determine the yield normalized deviatoric particle force state. We make a cut through half of the particle, determine the three components of force for each pd-bond, and then sum up the force components for each direction,

$$\{F_p\} = \begin{Bmatrix} F_x \\ F_y \\ F_z \end{Bmatrix} = \begin{Bmatrix} F_{1,x} + F_{3,x} + F_{5,x} + \cdots + F_{13,x} + F_{15,x} + F_{17,x} \\ F_{1,y} + F_{3,y} + F_{5,y} + \cdots + F_{13,y} + F_{15,y} + F_{17,y} \\ F_{1,z} + F_{3,z} + F_{5,z} + \cdots + F_{13,z} + F_{15,z} + F_{17,z} \end{Bmatrix} = \begin{Bmatrix} f_y \\ 0 \\ 0 \end{Bmatrix}. \quad (6.10)$$

Note that all the 'odd' number pd-bonds have been used (for a total of nine pd-bonds) to find the particle force state. Because we have assumed uniaxial conditions the out-of-axis particles forces must sum to zero and the in-axis force must sum to pd-bond yield force, f_y. We then use Equation 6.6 to solve for the average force state of the particle,

$$F_{Avg} = \frac{f_y + 0 + 0}{3} = \frac{1}{3} f_y. \quad (6.11)$$

Substituting Equations 6.10 and 611 into Equation 6.7 we then find the normalized deviatoric particle force state,

$$F_{NormDev} = \sqrt{\left(F_x - F_{Avg}\right)^2 + \left(F_y - F_{Avg}\right)^2 + \left(F_z - F_{Avg}\right)^2},$$

$$F_{NormDev} = \sqrt{\left(f_y - \frac{1}{3} f_y\right)^2 + \left(0 - \frac{1}{3} f_y\right)^2 + \left(0 - \frac{1}{3} f_y\right)^2},$$

$$F_{NormDev} = \sqrt{\frac{4}{9} {f_y}^2 + \frac{1}{9} {f_y}^2 + \frac{1}{9} {f_y}^2},$$

$$F_{NormDev} = \sqrt{\frac{2}{3}} f_y. \quad (6.12)$$

Therefore, under any loading, we assume that a SPLM particle will yield when the normalized deviatoric particle force state equals or exceeds the square root of two thirds times the pd-bond yield force,

$$F_{NormDev} \geq \sqrt{\frac{2}{3}} f_y, \quad (6.13)$$

6.3 SPLM plastic stretch rate

The total SPLM pd-bond stretch state, $\{\boldsymbol{S^T}\}$, can be separated into two parts: the elastic pd-bond stretch state, $\{\boldsymbol{S^e}\}$, and plastic pd-bond stretch state, $\{\boldsymbol{S^p}\}$,

$$\{\boldsymbol{S^T}\} = \{\boldsymbol{S^e}\} + \{\boldsymbol{S^p}\}. \tag{6.14}$$

The pd-bond force state is only a function of the elastic pd-bond stretch state, thus we rearrange Equation 6.14 as

$$\{\boldsymbol{S^e}\} = \{\boldsymbol{S^T}\} - \{\boldsymbol{S^p}\}. \tag{6.15}$$

Before the particle equals or exceeds the yield criteria, the elastic pd-bond stretch state is equal to the total pd-bond stretch state. However, once the yield criteria is met we now must subtract out the plastic pd-bond stretch state from the total pd-bond stretch state to find the pd-bond force state. Therefore we must define a *plastic pd-bond stretch rate* to solve for the plastic pd-bond stretch.

We begin with the Prandtl-Reuss equations from classical mechanics. They assume that at any instant the plastic strain deviation rate, $\dot{\varepsilon}^p$, is proportional to the deviatoric stress, $\boldsymbol{\sigma'}$, at that instant,

$$\frac{\dot{\varepsilon}^p_{xx}}{\sigma'_{xx}} = \frac{\dot{\varepsilon}^p_{yy}}{\sigma'_{yy}} = \frac{\dot{\varepsilon}^p_{zz}}{\sigma'_{zz}} = \frac{\frac{1}{2}\dot{\gamma}^p_{xy}}{\tau_{xy}} = \frac{\frac{1}{2}\dot{\gamma}^p_{yz}}{\tau_{yz}} = \frac{\frac{1}{2}\dot{\gamma}^p_{zx}}{\tau_{zx}} = \lambda. \tag{6.16}$$

where λ is a non-negative constant. Equation 6.16 can be expressed in matrix form in terms of the actual (not the deviatoric) stresses,

$$\{\dot{\boldsymbol{\varepsilon}}^{\boldsymbol{p}}\} = \lambda[Q]\{\boldsymbol{\sigma}\} \tag{6.17}$$

or

$$\begin{Bmatrix} \dot{\varepsilon}_{xx}^{p} \\ \dot{\varepsilon}_{yy}^{p} \\ \dot{\varepsilon}_{zz}^{p} \\ \dot{\gamma}_{xy}^{p} \\ \dot{\gamma}_{yz}^{p} \\ \dot{\gamma}_{zx}^{p} \end{Bmatrix} = \lambda \begin{bmatrix} 2/3 & -1/2 & -1/2 & 0 & 0 & 0 \\ -1/2 & 2/3 & -1/2 & 0 & 0 & 0 \\ -1/2 & -1/2 & 2/3 & 0 & 0 & 0 \\ 0 & 0 & 0 & 2 & 0 & 0 \\ 0 & 0 & 0 & 0 & 2 & 0 \\ 0 & 0 & 0 & 0 & 0 & 2 \end{bmatrix} \begin{Bmatrix} \sigma_{xx} \\ \sigma_{yy} \\ \sigma_{zz} \\ \tau_{xy} \\ \tau_{yz} \\ \tau_{zx} \end{Bmatrix},$$

where

$$[Q] = \begin{bmatrix} 2/3 & -1/2 & -1/2 & 0 & 0 & 0 \\ -1/2 & 2/3 & -1/2 & 0 & 0 & 0 \\ -1/2 & -1/2 & 2/3 & 0 & 0 & 0 \\ 0 & 0 & 0 & 2 & 0 & 0 \\ 0 & 0 & 0 & 0 & 2 & 0 \\ 0 & 0 & 0 & 0 & 0 & 2 \end{bmatrix}. \tag{6.18}$$

To emphasize, Equation 6.17 shows the relationship between stress and *plastic strain rate*, not the plastic strain. Beyond the elastic limit, the total strain, ε^T, is now the sum of the elastic strain, ε^e, and the plastic strain, ε^p,

$$\varepsilon_{total} = \varepsilon^e + \varepsilon^p. \tag{6.19}$$

Furthermore, the stress components in Equation 6.17 are only a function of the elastic strain and *not* the total strain. If the stress is known for a given time step, $\mathrm{d}t$, then the plastic strain rate, $(\dot{\varepsilon}^p)_i$, can be determined from Equation 6.17. Thus the plastic strain for that time step, $(\varepsilon^p)_i$, is

$$(\varepsilon^p)_i = (\dot{\varepsilon}^p)_i \cdot \mathrm{d}t \tag{6.20}$$

and the total plastic strain is the sum of plastic strains for n time steps

$$\varepsilon^p = \sum_{i=1}^{n} (\varepsilon^p)_i. \tag{6.21}$$

Thus the plastic strain will increase for every time step that the material is yielding.

The plastic strain rate is governed by the plastic flow constant, λ. In SPLM λ is a model parameter chosen by the user, typically $1 > \lambda > 0$. The reason is because the flow rate is time dependent, therefore λ can be chosen to limit plastic flow for each time step and ensuring that plastic deformation does not create undesirable results. If plastic deformation occurs to quickly it may cause instability in the model. On the other hand, if plastic deformation occurs to slowly the material will behave as a visco-plastic material and not the desired elastic-perfectly plastic behavior.

Recall from Chapter 4 that an equivalent SPLM pd-bond stretch state can be expanded from the classical strain using $[N]$,

$$\{\boldsymbol{S}\} = [N]\{\boldsymbol{\varepsilon}\}, \tag{4.5}$$

and that a pd-bond force state can be reduced to an equivalent classical stress using $[M]$,

$$\{\boldsymbol{\sigma}\} = [M]\{\boldsymbol{T}\}. \tag{4.6}$$

We showed in Chapter 4 that $[N]$ is a kinematic relationship between strain and stretch states as a function of direction cosines. Therefore, $[N]$ will also expand the pd-bond plastic stretch state rate, $\dot{S}^p$, from classical plastic strain rate,

$$\{\dot{\boldsymbol{S}}^{\boldsymbol{p}}\} = [N]\{\dot{\boldsymbol{\varepsilon}}^{\boldsymbol{p}}\}. \tag{6.22}$$

Pre-multiplying both sides of Equation 6.16 by $[N]$ yields

$$\{\dot{\boldsymbol{S}}^{\boldsymbol{p}}\} = \lambda[N][Q]\{\boldsymbol{\sigma}\}. \tag{6.23}$$

Then by substituting Equation 4.6 for $\{\boldsymbol{\sigma}\}$, Equation 6.23 becomes

$$\{\boldsymbol{S^p}\} = \lambda[N][Q][M]\{\boldsymbol{T}\}. \tag{6.24}$$

Therefore, the SPLM pd-bond plastic stretch rate is a function of the elastic pd-bond force state of a particle,

$$\{\boldsymbol{S^p}\} = \lambda[R]\{\boldsymbol{T}\} \tag{6.25}$$

where $[R]$ is

$$[R] = [N][Q][M] \tag{6.26}$$

and λ is chosen by the user. Substituting Equations 4.25, 4.27, and 6.18 into Equation 6.26 yields

$$[R] = \frac{\sqrt{2}}{24L^2}\begin{bmatrix}
8 & 8 & -1 & -1 & -1 & -1 & -1 & -1 & -1 & -1 & -4 & -4 & \cdots \\
8 & 8 & -1 & -1 & -1 & -1 & -1 & -1 & -1 & -1 & -4 & -4 & \cdots \\
-1 & -1 & 8 & 8 & -1 & -1 & -1 & -1 & -4 & -4 & -1 & -1 & \cdots \\
-1 & -1 & 8 & 8 & -1 & -1 & -1 & -1 & -4 & -4 & -1 & -1 & \cdots \\
-1 & -1 & -1 & -1 & 8 & 8 & -4 & -4 & -1 & -1 & -1 & -1 & \cdots \\
-1 & -1 & -1 & -1 & 8 & 8 & -4 & -4 & -1 & -1 & -1 & -1 & \cdots \\
-1 & -1 & -1 & -1 & -4 & -4 & 8 & 8 & -1 & -1 & -1 & -1 & \cdots \\
-1 & -1 & -1 & -1 & -4 & -4 & 8 & 8 & -1 & -1 & -1 & -1 & \cdots \\
-1 & -1 & -4 & -4 & -1 & -1 & -1 & -1 & 8 & 8 & -1 & -1 & \cdots \\
-1 & -1 & -4 & -4 & -1 & -1 & -1 & -1 & 8 & 8 & -1 & -1 & \cdots \\
-4 & -4 & -1 & -1 & -1 & -1 & -1 & -1 & -1 & -1 & 8 & 8 & \cdots \\
-4 & -4 & -1 & -1 & -1 & -1 & -1 & -1 & -1 & -1 & 8 & 8 & \cdots \\
2 & 2 & 2 & 2 & -4 & -4 & -4 & -4 & 2 & 2 & 2 & 2 & \cdots \\
2 & 2 & 2 & 2 & -4 & -4 & -4 & -4 & 2 & 2 & 2 & 2 & \cdots \\
-4 & -4 & 2 & 2 & 2 & 2 & 2 & 2 & 2 & 2 & -4 & -4 & \cdots \\
-4 & -4 & 2 & 2 & 2 & 2 & 2 & 2 & 2 & 2 & -4 & -4 & \cdots \\
2 & 2 & -4 & -4 & 2 & 2 & 2 & 2 & -4 & -4 & 2 & 2 & \cdots \\
2 & 2 & -4 & -4 & 2 & 2 & 2 & 2 & -4 & -4 & 2 & 2 & \cdots
\end{bmatrix}$$

$$\begin{bmatrix}
\cdots & 2\sqrt{2} & 2\sqrt{2} & -4\sqrt{2} & -4\sqrt{2} & 2\sqrt{2} & 2\sqrt{2} \\
\cdots & 2\sqrt{2} & 2\sqrt{2} & -4\sqrt{2} & -4\sqrt{2} & 2\sqrt{2} & 2\sqrt{2} \\
\cdots & 2\sqrt{2} & 2\sqrt{2} & 2\sqrt{2} & 2\sqrt{2} & -4\sqrt{2} & -4\sqrt{2} \\
\cdots & 2\sqrt{2} & 2\sqrt{2} & 2\sqrt{2} & 2\sqrt{2} & -4\sqrt{2} & -4\sqrt{2} \\
\cdots & -4\sqrt{2} & -4\sqrt{2} & 2\sqrt{2} & 2\sqrt{2} & 2\sqrt{2} & 2\sqrt{2} \\
\cdots & -4\sqrt{2} & -4\sqrt{2} & 2\sqrt{2} & 2\sqrt{2} & 2\sqrt{2} & 2\sqrt{2} \\
\cdots & -4\sqrt{2} & -4\sqrt{2} & 2\sqrt{2} & 2\sqrt{2} & 2\sqrt{2} & 2\sqrt{2} \\
\cdots & -4\sqrt{2} & -4\sqrt{2} & 2\sqrt{2} & 2\sqrt{2} & 2\sqrt{2} & 2\sqrt{2} \\
\cdots & 2\sqrt{2} & 2\sqrt{2} & 2\sqrt{2} & 2\sqrt{2} & -4\sqrt{2} & -4\sqrt{2} \\
\cdots & 2\sqrt{2} & 2\sqrt{2} & 2\sqrt{2} & 2\sqrt{2} & -4\sqrt{2} & -4\sqrt{2} \\
\cdots & 2\sqrt{2} & 2\sqrt{2} & -4\sqrt{2} & -4\sqrt{2} & 2\sqrt{2} & 2\sqrt{2} \\
\cdots & 2\sqrt{2} & 2\sqrt{2} & -4\sqrt{2} & -4\sqrt{2} & 2\sqrt{2} & 2\sqrt{2} \\
\cdots & 8\sqrt{2} & 8\sqrt{2} & -4\sqrt{2} & -4\sqrt{2} & -4\sqrt{2} & -4\sqrt{2} \\
\cdots & 8\sqrt{2} & 8\sqrt{2} & -4\sqrt{2} & -4\sqrt{2} & -4\sqrt{2} & -4\sqrt{2} \\
\cdots & -4\sqrt{2} & -4\sqrt{2} & 8\sqrt{2} & 8\sqrt{2} & -4\sqrt{2} & -4\sqrt{2} \\
\cdots & -4\sqrt{2} & -4\sqrt{2} & 8\sqrt{2} & 8\sqrt{2} & -4\sqrt{2} & -4\sqrt{2} \\
\cdots & -4\sqrt{2} & -4\sqrt{2} & -4\sqrt{2} & -4\sqrt{2} & 8\sqrt{2} & 8\sqrt{2} \\
\cdots & -4\sqrt{2} & -4\sqrt{2} & -4\sqrt{2} & -4\sqrt{2} & 8\sqrt{2} & 8\sqrt{2}
\end{bmatrix}. \tag{6.27}$$

Therefore, we can now calculate the plastic pd-bond stretch rate for time step i, $\{\dot{\boldsymbol{S}}^{\boldsymbol{p}}\}_{\boldsymbol{i}}$, from the pd-bond force state. The plastic pd-bond stretch state for time step i, $\{\boldsymbol{S}^{\boldsymbol{p}}\}_{\boldsymbol{i}}$, is $\{\dot{\boldsymbol{S}}^{\boldsymbol{p}}\}_{\boldsymbol{i}}$ multiplied by the duration of the time step, dt,

$$\{\boldsymbol{S}^{\boldsymbol{p}}\}_{\boldsymbol{i}} = \{\dot{\boldsymbol{S}}^{\boldsymbol{p}}\}_{\boldsymbol{i}} dt \tag{6.28}$$

The total plastic pd-bond stretch it the sum of all the plastic pd-bond stretches for n time steps,

$$\{\boldsymbol{S}^{\boldsymbol{p}}\} = \sum_{i=1}^{n} \{\boldsymbol{S}^{\boldsymbol{p}}\}_{\boldsymbol{i}}. \tag{6.29}$$

Note that $\{\boldsymbol{S}^{\boldsymbol{p}}\}$ represents the permanent deformation of the particle (i.e. it will not be recovered when the loads are removed).

6.4 Summary

This now defines our SPLM plasticity model. In this chapter we have defined a yield criterion for a SPLM particle as well as a SPLM plastic stretch flow rule to model deformation beyond the elastic limit. However, when testing the yield criterion, we observed that SPLM particles began yielding at lower than expected pd-bond force states. The author concludes that there must be a flaw in is approach for determining a SPLM particle yield state and more research is needed. This approach for determining a SPLM yield criteria has been included with the hope that future researchers will not make the same mistakes as the author.

The author does claim that the SPLM pd-bond flow rule is still valid. We derived our flow rule from the Prandtl-Reuss equations based on kinematic and energy equivalence. The author believes that the assumptions made in developing the SPLM pd-bond flow rule are less subjective than the assumptions make for the SPLM yield criteria. However to be clear, this is the author's opinion and cannot be proven until a valid SPLM yield criteria is developed.

Chapter 7

Examples

7.1 Introduction

In this chapter we will demonstrate the state-based peridynamic lattice model (SPLM) with several examples. To run our SPLM examples we use a program called 'pdQ2' written by Walter Gerstle, colleagues, and students. We then compare the SPLM results with the static classical analytical solutions. The examples shown in this chapter are for 'proof of concept' and are not intended to be an exhaustive proof of the validity SPLM.

Two examples will be shown to demonstrate SLPM linear elasticity: a one-dimensional bar subjected to uniaxial force and a two-dimensional plate under plane stress conditions subjected to unidirectional force. For each linear elastic example we will run three simulations, varying structural size of our models to see the effect on our results. Because pdQ2 is a dynamic model, the loading will begin at zero and ramp up gradually to the desired load. The load is then held constant so that all lingering vibrations are damped out and a quasi-static solution is obtained. From the final time step, the corresponding SPLM pd-bond stretch state for a predetermined particle is reduced to an equivalent classical strain. The SPLM results are then compared to the classical solution. A full convergence study will not be done in this thesis. The plasticity model is not implanted due to lack of time.

For both examples we consider the bar or plate to be a linear elastic material with a modulus of elasticity E, Poisson's ratio v, and a lattice spacing L as follows:

$$E = 24.86(10)^9 \frac{N}{m^2}, \tag{7.1}$$

$$v = 0.2, \tag{7.2}$$

and

$$L = 0.025\ m. \tag{7.3}$$

7.2 One-dimensional linear elastic bar subjected to uniaxial force

The first example uses the one-dimensional linear elastic SPLM relationships developed in Section 5.8 to model a bar under a state of uniaxial force. To model a bar, a representative strand of SPLM particles, with tributary area, $= \frac{L^2}{\sqrt{2}}$, is subjected to uniaxial loading. A force P of $1(10)^4$ Newtons is imposed on each end particle (shown in green in Figure 7.1) producing a state of uniaxial tensile force in the tributary strand of particles. Therefore, the corresponding classical stress is

$$\sigma_{xx} = \frac{P}{A} = \frac{1(10)^4 N}{(0.025m)^2/\sqrt{2}} = 22627417\frac{N}{m^2}. \tag{7.4}$$

Under these conditions, the classical mechanics relationship between stress, σ_{xx}, and elastic strain, ${\varepsilon_{xx}}^e$, is

$${\sigma_{xx} = E \cdot \varepsilon_{xx}}^e. \tag{7.5}$$

Thus, the classical strain is

$${\varepsilon_{xx}}^e = \frac{\sigma_{xx}}{E} = \frac{22627417\frac{N}{m^2}}{24.86(10)^9\frac{N}{m^2}} = 9.1019(10^{-4}). \tag{7.6}$$

Three lattice strands of differing lengths were modeled using pdQ2: $0.5m$, $1.0m$, and $2.0m$ long strands. The longer the strand, the more SPLM particles it contained. The number of particles used for each strand is shown in Table 7.1. The force was ramped up and held constant

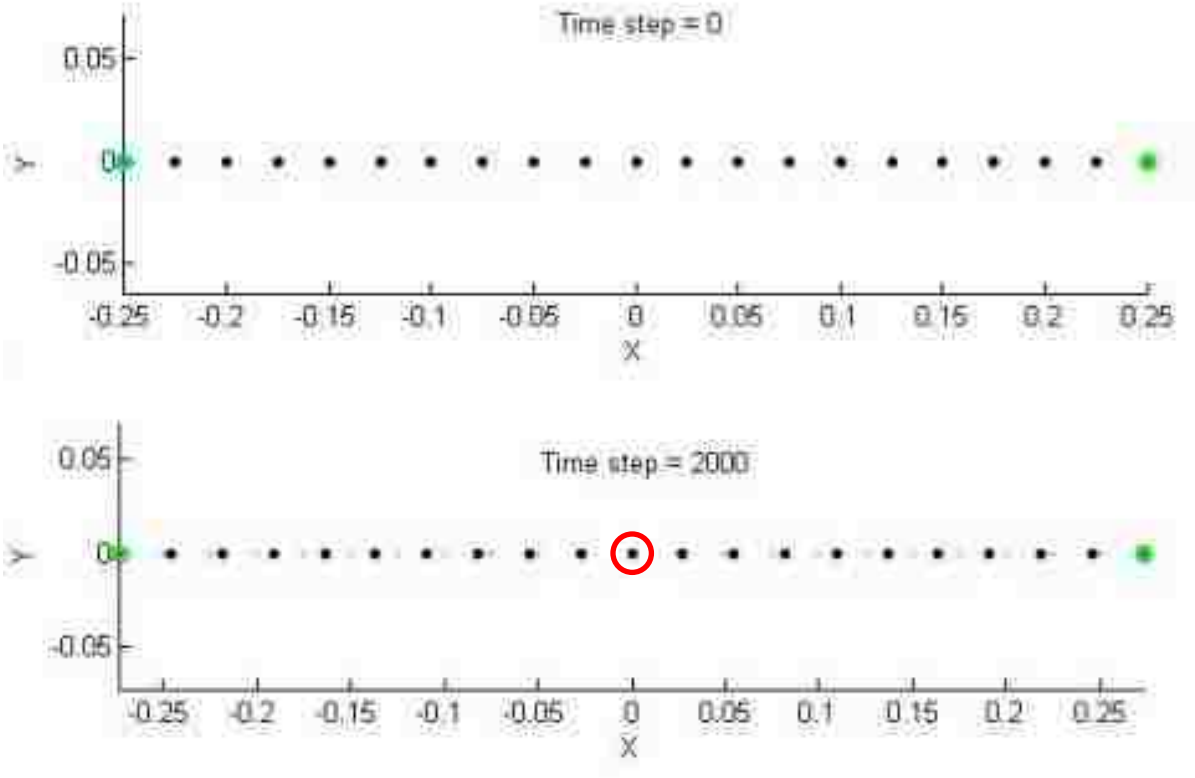

Figure 7.1 The reference configuration and deformed shape at 1000x magnification of a 0.5m lattice strand

for each strand over 2000 time steps to ensure that a static solution was reached. The duration of the time step was determined using the procedure outlined in [11]. On the last time step the center particle's (circled in red in figure 7.1) pd-bond stretch state is reduced to its equivalent strain. The center particle was chosen so as to reduce any boundary effects on our results. We then found the percent difference between the classical strain and the equivalent SPLM strain,

$$(\%\ Diff) = \frac{\varepsilon_{classic} - \varepsilon_{SPLM}}{\varepsilon_{classic}}. \tag{7.7}$$

The results of these three simulations are shown in Table 7.1.

$length\ (m)$	$Number\ of\ Particles$	$(\varepsilon_{xx})_{classic}$	$(\varepsilon_{xx})_{SPLM}$	$(\%\ Diff)_x$
0.5	21	$9.1019(10^{-4})$	$9.1046(10^{-4})$	-0.03%
1.0	41	$9.1019(10^{-4})$	$9.1079(10^{-4})$	-0.07%
2.0	81	$9.1019(10^{-4})$	$9.1038(10^{-4})$	-0.02%

Table 7.1, Percent difference between uniaxial $(\varepsilon_{xx})_{classic}$ and $(\varepsilon_{xx})_{SPLM}$

From these results, we see that SPLM gives virtually the same results as the classical model in the case of uniaxial force. It appears that the structural size of the strand does not have any systematic effect on the SPLM results; however more testing must be done to confirm this observation. The source of the small errors has not been investigated.

7.3 Two-dimensional plate under linear elastic plane stress conditions

The second example uses the linear elastic plane stress SPLM relationships developed in Section 5.9 to model a plate subjected to unidirectional force. To model a plate, a representative layer of particles, with thickness, $= \sqrt{\frac{2}{3}}L$, is subjected to unidirectional force. A force of $1(10)^4$ Newtons is imposed on each particle on the left and right boundaries of the plate (shown in green in Figure 7.2) producing a state of unidirectional tensile force in the tributary layer of particles. Thus the total force P on the layer of particles is the number of rows of particles, N_{rows}, times the force,

$$P = N_{rows} \cdot 1(10)^4 \tag{7.8}$$

The total width w of the layer of particles is the number of rows of particles, N_{rows}, times the tributary width, $\frac{\sqrt{3}}{2}L$, of a SPLM particle,

$$w = N_{rows} \cdot \frac{\sqrt{3}}{2}L. \tag{7.9}$$

Therefore, the area A normal to the force is the total width times the thickness of the layer,

$$A = w \cdot t = N_{rows} \cdot \frac{\sqrt{3}}{2}L \cdot \sqrt{\frac{2}{3}}L = N_{rows} \cdot \frac{L^2}{\sqrt{2}}. \tag{7.10}$$

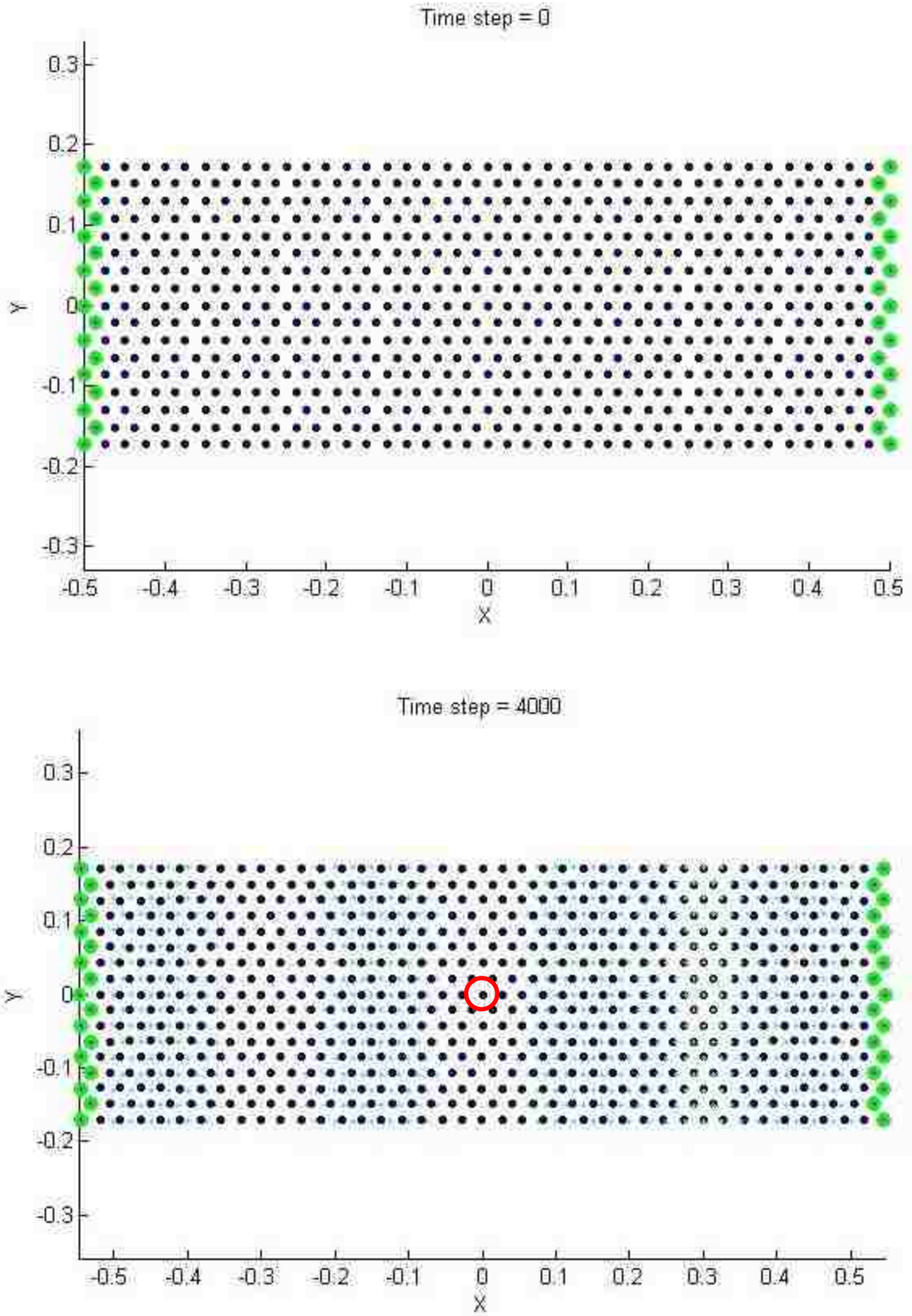

Figure 7.2 The reference configuration and deformed shape at 100x magnification of a 40 particle long by 16 particle wide lattice layer

The equivalent classical stress in the horizontal direction is then

$$\sigma_{xx} = \frac{P}{A} = \frac{N_{rows} \cdot 1(10)^4 N}{N_{rows} \cdot (0.025m)^2/\sqrt{2}} = 22627417 \frac{N}{m^2}, \tag{7.11}$$

and the classical strain is

$$\varepsilon_{xx}{}^{e} = \frac{\sigma_{xx}}{E} = \frac{22627417 \frac{N}{m^2}}{24.86(10)^9 \frac{N}{m^2}} = 9.1019(10^{-4}). \tag{7.12}$$

Assuming plane stress conditions and that $\sigma_{yy} = 0$, the corresponding vertical strain is

$$\varepsilon_{yy}{}^{e} = -\nu \cdot \varepsilon_{xx}{}^{e},$$

$$\varepsilon_{yy}{}^{e} = -0.2 \cdot 9.1019(10^{-4}),$$

$$\varepsilon_{yy}{}^{e} = -1.8204(10^{-4}). \tag{7.13}$$

Three different sized layers of particles were modeled in pdQ2: 10 particles (0.25m) long by 4 particles (0.0217m) wide, 20 particles (0.5m) long by 8 particles (0.1732m) wide, and 40 particles (1.0m) long by 16 particles (0.3464m) wide. The total number of particles used for each layer is shown in Table 7.2 and Table 7.3. The force was ramped up and held constant for each layer over 4000 time steps to ensure that a quasi-static solution was reached. Just as in the one-dimensional case, on the last time step the center particle's (circled in red in figure 7.2) pd-bond stretch state is reduced to its equivalent strain. The percent difference between the classical strain and the equivalent SPLM strain for each example is recorded in Tables 7.2 and 7.3.

$length\ (m)$	$width\ (m)$	$Number\ of\ Particles$	$(\varepsilon_{xx})_{classic}$	$(\varepsilon_{xx})_{SPLM}$	$(\%\ Diff)_x$
0.25	0.0217	49	$9.1019(10^{-4})$	$8.9553(10^{-4})$	1.61%
0.5	0.1732	169	$9.1019(10^{-4})$	$9.0186(10^{-4})$	0.92%
1.0	0.3464	625	$9.1019(10^{-4})$	$9.0527(10^{-4})$	0.54%

Table 7.2, Percent difference between plane stress $(\varepsilon_{xx})_{classic}$ and $(\varepsilon_{xx})_{SPLM}$

$length\,(m)$	$width\,(m)$	$Number\ of\ Particles$	$(\varepsilon_{yy})_{classic}$	$(\varepsilon_{yy})_{SPLM}$	$(\%\ Diff)_y$
0.25	0.0217	49	$-1.8204(10^{-4})$	$-1.8043(10^{-4})$	0.89%
0.5	0.1732	169	$-1.8204(10^{-4})$	$-1.8042(10^{-4})$	0.89%
1.0	0.3464	625	$-1.8204(10^{-4})$	$-1.8104(10^{-4})$	0.55%

Table 7.3, Percent difference between plane stress $(\varepsilon_{yy})_{classic}$ and $(\varepsilon_{yy})_{SPLM}$

From these three tests, we see that SPLM results are very close to the classical model in the case of plane stress unidirectional force. Different from the one-dimensional case, the structural size of the layer does have a slight effect on the SPLM results; therefore a convergence study is indicated.

7.4 Summary

These two examples show that SPLM has the potential ability to model linear-elastic materials, producing similar or virtually identical results to the classical solution. Note that the word 'potential' is used and not 'conclusive'. More research and testing must be done to prove SPLM's capabilities to model linear elastic materials. However, the author does claim that these examples do succeed in showing a proof of concept for the SPLM theory developed in this thesis.

Chapter 8

Conclusion

8.1 Summary and Future Work

In this thesis we have presented the state-based peridynamic lattice model (SPLM). We began by going over a brief history of classical and peridynamic models, highlighting the strengths and weaknesses of each. With the knowledge of what other great minds have done before us, we began to define SPLM. SPLM is built from the basics of Newton's three laws of motion with alternate basic assumptions that are more suitable for the computer age.

We have shown that when there exists a spatially homogeneous strain field that a comparison between SPLM and classical mechanics can be made. This is crucially important because virtually all mechanics of materials models are in terms of stress and strain. Therefore with the expansion and reduction tools developed in chapter four, SPLM is more relevant to the engineering world. Particle pd-bond force states and stretch states, which have little to no meaning to the average engineer, can now be expressed in terms of stress and strain. This provides a bridge for SPLM to be used in engineering practice.

Surprisingly, we discovered in this research that there are an infinite number of possible constitutive relationships between pd-bond force and stretch state that will ensure isotropy and identical macro-elastic behavior in comparison with the classical model. We have presented several possible linear elastic constitutive solutions in this thesis. The examples conducted using these relationships show that SPLM can potentially be used to model linear elastic solids. More research is needed is to solve for the full three-dimensional and two-dimensional plane strain relationships.

We have presented one possible SPLM plasticity model in this thesis. The author is confident that with time, more research, and a fresh set of eyes, that a viable SPLM plasticity model will be developed.

An ultimate goal of SPLM is to model elasticity, plasticity, damage, and fracture in one all-inclusive model. To achieve this, the SPLM linear elastic model must be perfected and SPLM plasticity, damage, and fracture models must be developed. If this can be achieved, SPLM solid modeling may very well show itself to be the next great engineering tool.

References

[1] Anderson T. L., "Fracture Mechanics", 3rd Edition, Taylor and Francis Group, LLC, 2005

[2] Gerstle W. and Sau N., "Peridynamic Modeling of Concrete Structures", Proceedings of the Fifth International Conference on Fracture Mechanics of Concrete Structures, Li, Leung, Willam, and Billing, Eds., Ia-FRAMCOS, Vol. 2, pp. 949-956, 2004.

[3] Gerstle W., Sau N., and Silling S., "Peridynamic Modeling of Plain and Reinforced Concrete Structures", Proceedings of the 18th Intl. Conf. on Structural Mechanics in Reactor Technology (SMiRT 18), Atomic Energy Press, Beijing China, Aug. 7-12, 949-956, 2005.

[4] Gerstle W., Sau N., and Silling S., "Peridynamic Modeling of Concrete Structures", Nuclear Engineering and Design, 237(12-13): 1250-1258, 2007.

[5] Halliday D., Resnick R., Walker J, "Fundamentals of Physics", 7th Edition, John Wiley & Sons Inc., 2005.

[6] Mase G.E., Mase G.T., "Continuum Mechanics for Engineers", CRC Press Inc., 1992.

[7] Rahman, A., "Lattice-Based Peridynamic Modeling of Linear Elastic Solids", Abstract of Thesis, The University of New Mexico, Albuquerque, New Mexico, 2011.

[8] Silling S.A., "Reformulation of Elasticity Theory for Discontinuities and Long-Range Forces", Journal of the Mechanics and Physics of Solids, Vol. 48, pp. 175-209, 2000.

[9] Silling S., Epton M., Weckner O., Xu J., and Askari E., "Peridynamic States and Constitutive Modeling", Journal of Elasticity, Vol. 88, pp. 151-184, 2007.

[10] Solecki R., Conant R. J., "Advanced Mechanics of Materials", Oxford University Press, 2003.

[11] Taylor L., Flanagan D., "PRONTO 3D a three-dimensional transient solid dynamics program", SAND87-1912, Sandia National Laboratories, Albuquerque, New Mexico, 1989.

[12] Timoshenko S., "History of Strength of Materials", Courier Dover Publications, 1983.

[13] Warren T., Silling S., Askari A., Weckner O., Epton M., Xu J., "A non-ordinary state-based peridynamic method to model solid material deformation and fracture", International Journal of Solids and Structures, Vol. 46, pp. 1186-1195, 2009.

Appendix

*** Matlab code used to solve for SPLM linear elastic constants ***

```
function three_dimensional_a_b_c

clc
clear all

syms E L v a b c

D = (E/(-2*v^2-v+1))*[ 1-v  v    0          v    0          0          ;
                       v    1-v  0          v    0          0          ;
                       0    0    (1-2*v)/2  0    0          0          ;
                       v    v    0          1-v  0          0          ;
                       0    0    0          0    (1-2*v)/2  0          ;
                       0    0    0          0    0          (1-2*v)/2 ];

Vol = L^3/sqrt(2);

R = [    L,                0,                       0; %1
        -L,                0,                       0; %2
       L/2,    (3^(1/2)*L)/2,                       0; %3
      -L/2,   -(3^(1/2)*L)/2,                       0; %4
      -L/2,    (3^(1/2)*L)/2,                       0; %5
       L/2,   -(3^(1/2)*L)/2,                       0; %6
       L/2,    (3^(1/2)*L)/6,  (2^(1/2)*3^(1/2)*L)/3; %7
      -L/2,   -(3^(1/2)*L)/6, -(2^(1/2)*3^(1/2)*L)/3; %8
      -L/2,    (3^(1/2)*L)/6,  (2^(1/2)*3^(1/2)*L)/3; %9
       L/2,   -(3^(1/2)*L)/6, -(2^(1/2)*3^(1/2)*L)/3; %10
         0,   -(3^(1/2)*L)/3,  (2^(1/2)*3^(1/2)*L)/3; %11
         0,    (3^(1/2)*L)/3, -(2^(1/2)*3^(1/2)*L)/3; %12
        -L,   -(3^(1/2)*L)/3,  (2^(1/2)*3^(1/2)*L)/3; %13
         L,    (3^(1/2)*L)/3, -(2^(1/2)*3^(1/2)*L)/3; %14
         0,  (2*3^(1/2)*L)/3,  (2^(1/2)*3^(1/2)*L)/3; %15
         0, -(2*3^(1/2)*L)/3, -(2^(1/2)*3^(1/2)*L)/3; %16
         L,   -(3^(1/2)*L)/3,  (2^(1/2)*3^(1/2)*L)/3; %17
        -L,    (3^(1/2)*L)/3, -(2^(1/2)*3^(1/2)*L)/3];%18

% Build N and Li
N = sym(zeros(18,6));
Li = sym(zeros(18,18));
```

```
for j = 1:18 % Get Direction Cosines
    Length = sqrt( R(j,1)^2 + R(j,2)^2 + R(j,3)^2 );
    if Length == (L^2)^(1/2)
        Length = L;
    else
        Length = 2^(1/2)*L;
    end
    N(j,:) = [ (R(j,1)/Length)^2 (R(j,2)/Length)^2 ...
               (R(j,1)/Length)*(R(j,2)/Length) (R(j,3)/Length)^2  ...
               (R(j,2)/Length)*(R(j,3)/Length) ...
               (R(j,3)/Length)*(R(j,1)/Length) ];
    Li(j,j) = Length;
end

N = simple(N);

M = simple((1/(2*Vol))*transpose(N)*Li);

% Build K
K = sym(zeros(18,18));
for i = 1:18
    for j = 1:18
        if i == j
            if i <= 12
                K(i,j) = a+b/12;
            else
                K(i,j) = c;
            end
        elseif ( (i ~= j) && (i <= 12) && (j <=12) )
            K(i,j) = b/12;
        else
            K(i,j) = 0;
        end
    end
end

K = K

D_eq = simple(M*K*N)

Eq1 = D(1,1) - D_eq(1,1);
Eq2 = D(4,4) - D_eq(4,4);
Eq3 = D(5,5) - D_eq(5,5);
sol = solve(Eq1, Eq2, Eq3, a, b, c);
a_s = simple(sol.a);
b_s = simple(sol.b);
c_s = simple(sol.c);
a = simple(eval(a_s))
b = simple(eval(b_s))
c = simple(eval(c_s))

end
```